1964

Electron diffraction investigation of O2, N2(CF3)4, and deuterium isotope effects in C2H6 and CH3NH2

Harlan Kieth Higginbotham
Iowa State University

ELECTRON DIFFRACTION INVESTIGATION OF O_2, $N_2(CF_3)_4$, AND DEUTERIUM ISOTOPE EFFECTS IN C_2H_6 and CH_3NH_2

by

Harlan Kieth Higginbotham

A Dissertation Submitted to the
Graduate Faculty in Partial Fulfillment of
The Requirements for the Degree of
DOCTOR OF PHILOSOPHY

Major Subject: Physical Chemistry

Approved:

Signature was redacted for privacy.

In Charge of Major Work

Signature was redacted for privacy.

Head of Major Department

Signature was redacted for privacy.

Dean of Graduate College

Iowa State University
Of Science and Technology
Ames, Iowa

1964

TABLE OF CONTENTS

I. INTRODUCTION

A. Purpose

In the present research, electron diffraction methods were employed to determine structural parameters of some hydrides and their deuterated analogs in order to observe magnitudes of primary and secondary isotope effects. Molecules studied for this purpose were ethane, deuterated ethane, methylamine, and deuterated methylamine. In another phase of this work oxygen and perfluorotetramethylhydrazine were investigated also.

Of the interatomic linkages studied to date, the CC single bond has perhaps been the favorite subject. The variation of this bond distance with respect to environment is well documented and many factors have been proposed to account for these differences (1). Until recently the most neglected of these factors has been the influence of nonbonded interactions. Bartell (2 - 6) has shown that various trends in bond lengths and other molecular properties can be accounted for by a steric model, including certain well-known secondary isotope effects in kinetic studies when deuterium is substituted for hydrogen. The steric model also leads to the prediction that secondary isotope effects on molecular structure should occur. These have never been studied heretofore. The existence of such effects would have important consequences in analyses of molecular structure by

spectroscopic techniques in which liberal use is made of deuterium substitution.

Ethane and methylamine were selected for this study principally because of the large number of nonbonded hydrogen or deuterium interactions occurring across the central bond.

Another important aspect of the hydride investigation is the further documentation of bond lengths. The CC and CH distances in ethane are often used as standards for theoretical purposes. The absolute significance of the operational parameters reported in previous ethane determinations has never been unambiguously stated. In addition, the need for accurate standards necessitates continued study by all methods.

In order to observe small differences in bond distances, such as secondary isotope effects, interpretational uncertainties associated with zero point vibrations must be taken into account. A precise electron diffraction study of diatomic molecules has been undertaken in this laboratory to test the validity of current interpretational schemes (7). Oxygen was among the molecules studied and is included in the present research.

Perfluorotetramethylhydrazine was selected for study as it offered an interesting steric problem. The nearest approach of fluorine atoms bonded to different atoms has been

regularly reported to be approximately twice the fluorine van der Waals radius of 1.35Å assigned by Pauling (8). Sometimes appreciable deformations of bonds are encountered in molecules with close approaches between fluorine atoms as they distort to increase F···F distances to 2.7Å. For example, atoms attached to double-bonded carbon atoms are usually found to lie in the same plane in unstrained molecules. In hexafluoropropene, however, they have been found to be out of plane (9). Polyethylene polymers are planar zigzag chains (10), while polytetrafluoroethylene are twisted into helical zigzag chains to relieve fluorine interactions (11). If angles in perfluorotetramethylhydrazine are assumed to be the same as the analogous angles in hydrazine (12) and CF_3 groups are tetrahedral with normal conformations, it is readily calculated that the nearest approach of fluorines is 1.78Å. Since this is considerably below the van der Waals diameter, it is of interest to determine the configuration achieved by this molecule as it deforms to minimize its energy.

B. Review of the Molecules

Ethane has been subjected to intermittent study by spectroscopic methods since 1905, when the infrared spectrum was observed by Coblentz (13). Subsequent studies were carried out by Levin and Meyer (14), Crawford (15), and Stitt (16). Wierl (17) first determined structural

parameters of ethane in 1932 by the electron diffraction method. Other early electron diffraction work was done by Bauer (18), Pauling and Brockway (19), and Hedberg and Shomaker (20). Structural parameters from spectroscopic work were first reported by Smith (21) and Hansen and Dennison (22).

More recent investigations of ethane include electron diffraction work by Almenningen and Bastiansen (23), and spectroscopic work by Stoicheff (24), and Lafferty and Plyler (25, 26).

Preliminary spectroscopic studies of methylamine were carried out by Thompson and Skinner (27), Cleaves and Plyler (28), Kirby-Smith and Bonner (29, 30), and Bailey et al. (31), in 1938 and 1939. Parameters were reported in 1939 and 1940 by Thompson (32) and Owens and Barker (33).

Microwave measurements of methylamine were first reported by Hershberger and Turkevich (34) in 1947, Gordy (35) in 1948, and Edwards et al. (36) in 1949. Since then comprehensive investigations have been made by Lide (37 - 40), and Shimoda et al. (41 - 44). Similar structural parameters and rotational barriers have been reported in both works. Electron diffraction results for methylamine were reported by Shomaker (45) in 1950.

The structures of deuterated ethane and methylamine have not been determined but some of the spectroscopic work on the hydrides incorporates data from the spectra of the deuterides.

In none of the diffraction work was sufficient absolute accuracy achieved to be helpful in the present study of isotope effects. In all of the spectroscopic studies it was assumed that hydrides and deuterides had identical structural parameters.

The interatomic distance in oxygen was first reported by Ossenbrüggen (46) in 1928 from a study of its band spectra. Other early spectroscopic investigations were carried out by Rassetti (47), and Curry and Herzberg (48). The bond length was also determined, though rather crudely, by gaseous x-ray diffraction in 1932 by Gajewski (49). Modern spectroscopic investigations include those by Babcock and Herzberg (50), Townes and Miller (51) and Tinkham and Strandberg (52). Karle (53) determined the interatomic distance by electron diffraction in 1955.

Preparation of perfluorotetramethylhydrazine was first reported in 1951 by Hazeldine (54). The infrared and nuclear magnetic resonance spectra have been observed by Young et al. (55). The latter disclosed all fluorines to be equivalent indicating an averaging over intramolecular motions in the time characteristic of NMR measurements. The molecule has not been subjected to an extensive structural analysis.

II. EXPERIMENTAL PROCEDURE

A. Apparatus

The experimental intensity data for this investigation were obtained using the rotating sector electron diffraction unit recently constructed at Iowa State University (Figure 1). It is similar in design to one at the University of Michigan (56) but the range of scattering angle is larger and the camera distance may be fixed more accurately. A discussion of the unit and experimental techniques is given below.

An electron beam, accelerated from a hot cathode gun by a potential of 40,000 volts, is focused by a magnetic lens and aligned by magnetic and electrostatic deflectors so that it passes through a small jet of the gas being studied. The gas is injected into the evacuated diffraction chamber through a small platinum nozzle by expansion from a large sample bulb. Sample bulb pressures ranged from 15 to 60 millimeters of mercury for this work. Three camera distances are available which make it possible to obtain overlapping data from $s = 3\text{Å}^{-1}$ to beyond $s = 60\text{Å}^{-1}$, where s is the scattering variable and equal to $(4\pi/\lambda)\sin\frac{1}{2}\phi$. Here λ is the electron wavelength and ϕ is the scattering angle. In the present work long and middle camera distances of 21.4 and 10.7 centimeters were used for obtaining data for all molecules. The short distance of 6.8 centimeters was used for oxygen and preliminary ethane data only. These distances were accurately

Figure 1. Front and side view of electron diffraction unit at Iowa State University

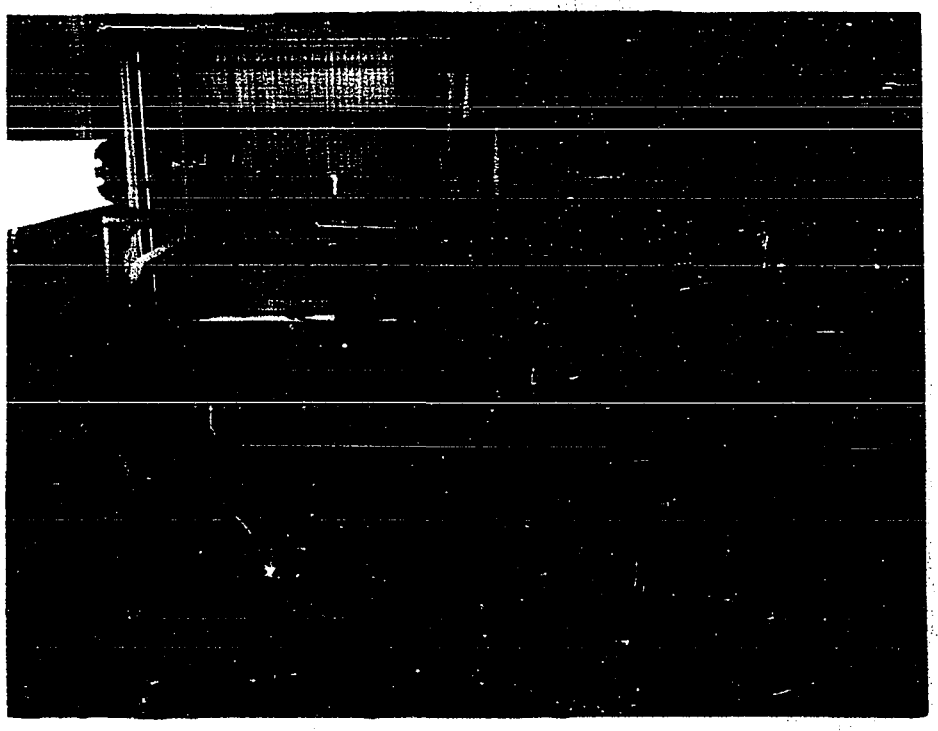

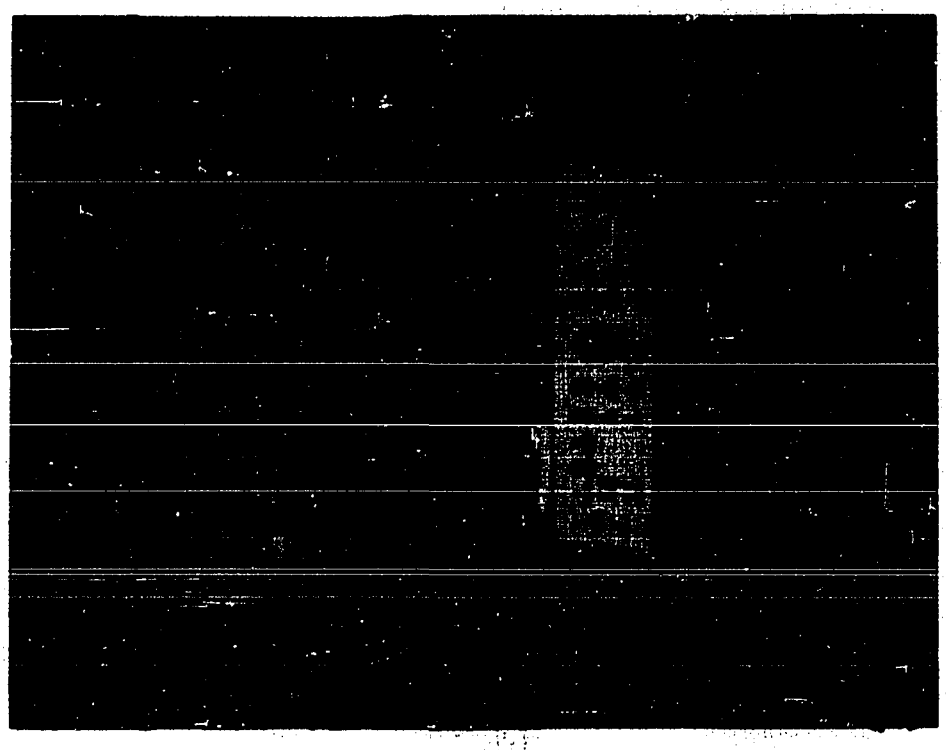

measured with a cathetometer. An electrostatic shutter is used in conjunction with an electrical timing device to obtain reproducible exposure times. The shutter and timer are both triggered by opening the stopcock of the sample bulb and after a preset time has elapsed the shutter automatically switches off the beam. Exposure times used ranged from 4 seconds to 30 seconds.

The diffracted intensity is recorded on fine grain photographic plates. Four by five inch Kodak process plates were used in this work. In order to measure accurately the diffracted intensity, its precipitous drop with increasing scattering variable, s, must be compensated for. This is accomplished by a sector rotating over the photographic plate which suitably screens the electrons before they strike the plate. For the present work a sector was employed in which the angular opening increased with the cube of the radius.

The optical densities of the oxygen plates were measured with a Leeds and Northrup recording microphotometer. Plates were centered on a rotating platform and spun at 600 rpm as they were scanned with the microphotometer. The spinning smooths grain irregularities and possible flaws in the photographic plates (57). Smooth, fine pencil lines were carefully drawn through the small random undulations of the recorded traces and optical densities were read, under magnification, at quarter-millimeter intervals from the center

of the plate. Densities may be read directly when using semi-log recording paper. This procedure is quite subjective and requires numerous manipulations. Consequently the procedure has been automated in an attempt to reduce subjectivity and manipulational errors. In the automated system the signal from the microphotometer was fed into a voltage to frequency converter which in turn was connected to a counter and digital recorder. The frequency, which is proportional to the voltage, was then recorded at each quarter millimeter interval as the rotating plate was positioned manually, using a precision screw. Measurements were made at regular time intervals to minimize errors arising from circuit drift, and were made in an uninterrupted sequence across the full diameter of the spinning plateholder. Optical densities were calculated from voltages by IBM 650 or IBM 7074 digital computers.

In both procedures, centering error and random scattering are manifested in a plot of $(D^R - D^L)$ versus r_{plate}, where D^R and D^L are optical densities from the right and left hand sides of the plateholder measured at a radius, r_{plate}, from the ascertained plate or trace center. A plate reading was considered acceptable when the overall scattering due to centering error was less than 0.4% and the random scattering due to microphotometer fluctuations did not exceed 0.1%.

B. Analysis of Data

1. Calculation of reduced intensity function

The fundamental equation representing the intensity due to the scattering of electrons by gaseous molecules, as derived by Debye (58), is

$$I(s) = \frac{A}{s^4} \left\{ \sum_k \left[(Z_k - F_k(s))^2 + S_k \right] + \sum_{i,j \neq i} \sum (Z_i - F_i(s))(Z_j - F_j(s)) \right.$$

$$\left. x \int_o^\infty P_{ij}(r) \frac{\sin sr}{sr} dr \right\} . \qquad (1)$$

The first term is due to atomic scattering, I_A, and the second due to molecular scattering, I_M,

where A is a constant,

s is the scattering variable $(4\pi/\lambda)\sin\frac{1}{2}\phi$,

Z_k is the atomic number of atom k,

F_k (s) is the coherent atom form factor of atom k,

S_k (s) is the incoherent atom factor of atom k,

$P_{ij}(r)$ is the probability distribution which describes the internuclear separation between the ijth atom pair.

It is common and convenient in electron diffraction structural investigations to study a ratio of I_M, the molecular scattering, to I_A, the atomic scattering. This ratio is referred to as the reduced molecular intensity function.

Dividing Equation 1 by I_A gives

$$\left[I(s)/I_A\right]-1 = \sum_i \sum_{j\neq i} \frac{(Z_i-F_j(s))\,(Z_j-F_j(s))}{\sum_k \left[(Z_k-F_k(s))^2+S_k(s)\right]} \int_o^\infty P_{ij}(r)\,\frac{\sin sr}{sr}\,dr$$

$$\text{or} \quad \left[I(s)/I_A\right] - 1 = I_M/I_A = M(s)_{th} \tag{2}$$

Equation 2 is more conveniently expressed as

$$M(s)_{th} = \sum_i \sum_{j\neq i} C_{ij}\mu_{ij}(s) \int_o^\infty P_{ij}(r)\,\frac{\sin sr}{sr}\,dr,$$

where C_{ij} is $Z_iZ_j / \sum_k (Z_k^2 + Z_k)$ and

$$\mu_{ij}(s) \text{ is } (Z_i-F_i(s))(Z_j-F_j(s)) \sum_k (Z_k^2 + Z_k) \,/$$

$$Z_iZ_j \sum_k \left[(Z_k-F_k(s))^2 + S_k(s)\right]$$

An experimental representation of M(s) can be obtained by dividing the observed intensity by a smooth background function, I_B, which is selected using certain criteria (59, 60), and subtracting one from the ratio.

$$M(s)_{exp} = (I(s)_{exp}/I_B)-1 \tag{3}$$

Usage of this ratio is the key to analysis of electron diffraction data. Direct comparison of $M(s)_{th}$ and $M(s)_{exp}$ is possible and, furthermore, structural information in the form of distribution curves, $P_{ij}(r)$, may be obtained by a Fourier inversion of Equation 2.

The calculations involved in obtaining intensity data from exposed photographic plates are discussed below. Three or four suitable plates for each camera distance were selected for microphotometering. Data obtained by the recording microphotometer were read directly as optical densities and mean optical densities were found by averaging D_i^R and D_i^L, which are the microphotometer chart readings for the ith point on the right hand side and left hand side respectively of the trace. The value obtained, $\bar{D}_i$, is then the mean optical density for the ith radial point. Averaging in this case sufficiently compensates for any monotonic drift. When the automated process was used, total optical densities were calculated from voltages. As the lamp source consisted of wet cell batteries, considerable voltage drift occurred over a long period of time and a correction was required. This drift was assumed to be monotonic and the mean optical densities were calculated by the equation

$$\bar{D}_i = (D_i^R + D_i^L)/2 - (1/4.6)\left[(\Delta V - V_0)/(V_M - V_0^f) + \Delta V_0/(V_R - V_0^i)\right] , \quad (4)$$

where D_i^R is $\log\left[(V_{100}^i - V_0^i)/(V_R - V_0^i)\right]$,

D_i^L is $\log\left[(V_{100}^i - V_0^i)/(V_L - V_0^i)\right]$,

ΔV_0 is $V_0^i - V_0^f$, ΔV is $V_R - V_L$ at r_{max},

V_M is V_R at $r = 43.75$ millimeters,

V_0^i and V_0^f are dark current voltages read before and after the plate was microphotometered, and

V_{100}^i is the voltage read when the light is passed through a clear portion of the plate.

As was previously mentioned, the criterion for a successfully microphotometered plate is the magnitude fluctuations in ΔD_i. For the recording method ΔD_i is simply taken to be the difference $D_i^R - D_i^L$; however, with the automated process a steady drift was taken into account, and ΔD_i was calculated by

$$\Delta D_i = (D_i^R - D_i^L) + (1/2.3)\left[(\Delta V - \Delta V_0)/(V_M - V_0^f) + \Delta V_0/(V_R - V_0)\right]\left[(r_i - r_{min})/(r_{max} - r_{min})\right] ,$$

where r_i is the radial distance corresponding to D_i^L and D_i^R, and r_{min} and r_{max} are respectively the smallest and largest radial distances used.

It should be noted that averaging of D_i^R and D_i^L minimizes the centering error in both procedures. However, a curve obtained by averaging two sinusoidal curves which are somewhat out of phase is slightly washed out. Therefore, it is the amount of reduction in amplitude that can be tolerated which determines the required centering accuracy.

Optical densities for each plate were converted to relative intensities by the equation

$$I_i = \bar{D}_i + \alpha \bar{D}_i^2 , \qquad (6)$$

where α is the emulsion calibration constant (61).

Intensities from plates of the same nozzle to plate distance were then averaged to give average intensities

$$\bar{I}_i = \sum_{j=i}^{N} I_{ij} E_j / N \qquad (7)$$

where I_{ij} is the intensity, from Equation 6, of the jth plate,

E_j is an exposure correction for putting individual plates on the same scale and

N is the number of plates to be averaged.

To correct for extraneous scattering a plate was exposed in the absence of gas and the extraneous intensity was represented analytically by

$$I_i^{ext} = \left[ar_i^2 + \alpha(ar_i^2)^2\right] E^{ext} \qquad (8)$$

where a is $D_{30}^{ext}/900$, in which D_{30}^{ext} is the optical density of the blank at r equal 30 millimeters and

E^{ext} is an exposure correction to put extraneous intensities on the same scale as experimental intensities.

Well leveled total intensities were then calculated from the expression

$$I_i(q)_T = \frac{(\bar{I}_i - I_i^{ext})\left[1+(r_i/L)^2\right]^{3/2}(\phi_i/r_i^3)}{\sum_k \left[(Z_k - F_k(q_i))^2 + S_k(q_i)\right]/q_i^4}, \qquad (9)$$

where $\left[1+(r_i/L)^2\right]^{3/2}$ is a correction for the inverse square fall off of the intensity on a flat photographic plate,

(ϕ_i/r_i^3) is a correction for the r cubed sector,

q_i[1] is the scattering variable calculated by $40 \sin \left[(\arctan r_i/L)/2\right]/\lambda$ in which L is the camera

---

[1] q is equal to $10s/\pi$. At one time, when computing facilities were rudimentary, it was more convenient to use than the variable s. At present it is used largely by force of habit as a carry-over from older computing programs.

distance, λ is the electron wavelength, and the denominator is the atomic intensity, I_A, which occurs in Equation 1.

The coherent and incoherent atom form factors, F(q) and S(q) respectively, were calculated at arbitrary q values using the following analytical expressions (62, 63)

$$F_k(q_i) = \sum_{n=1}^{N} a_n/(1 + b_n\, q_i^2)^1 n \qquad (11)$$

$$S_k(q) = A_k \left[1-0.200/(1+4.252V_{ik}^2) - 0.302/(1+9.907V_{ik}^2)^2 - 0.217/(1+31.9V_{ik}^2)^4 - 0.216/(1+108.2V_{ik}^2)^8\right] \qquad (12)$$

where A_k is a constant and

V_{ik} is $0.176\pi\ q_i/10\ Z_k^{2/3}$.

Experimental M(s) data were then obtained by drawing a smooth background, I_B, through the molecular oscillations of I(s) and computing values according to Equation 3. It is evident from Equation 9 that I_B ideally should be a straight line inasmuch as I(s) is the result of division by I_A. However, due to possible inadequacies of current theory, insufficient correction for extraneous scattering, variation of emulsion sensitivity, inaccuracies in the sector calibration, and perhaps unknown factors, I_B is usually nonlinear. Accordingly,

I_B can be considered a correction function which permits legitimate comparison of $M(s)_{th}$ and $M(s)_{exp}$.

2. Calculation and analysis of the radial distribution function

Electron diffraction data are reduced to molecular structure by two principal methods. These are: (a) the correlation method (64) in which experimental and theoretical reduced molecular intensities are compared and (b) the radial distribution method (65, 66) in which a Fourier inversion is performed on the $M(s)_{exp}$ function to give a radial distribution function, f(r). The latter method was applied almost exclusively in this investigation.

A radial distribution function can be obtained by a Fourier inversion of Equation 2 providing the coefficients $C_{ij}\mu_{ij}$ are constant and experimental data from s=0 to $s=\infty$ are available. Unfortunately neither condition is satisfied and the resulting limitations must be taken into account if accurate structural information is to be derived.

Several methods have been devised to account for the variation of the coefficient, μ_{ij} (67, 68, 69). The simplest precise technique which has been employed is, perhaps, that of Bartell et al. (69) in which a theoretical $\Delta M_c(s)$ function is subtracted from $M(s)_{exp}$ to give a constant coefficient reduced molecular intensity function, $M_c(s)_{exp}$. The function

$\triangle M_c(s)$ is the difference between $M(s)_{tn}$ and $M_c(s)_{tn}$ where $M_c(s)_{th}$ is calculated with μ_{ij} set equal to one.

Experimental intensity data were obtained in this study over the range from $s \simeq 3$ Å^{-1} to some upper limit s_{max}. Lack of data from $s=0$ to $s \simeq 3$ was taken into account by grafting calculated values of $M_c(s)_{th}$ onto the experimental curves to represent the missing data. Lack of data from s_{max} to $s=\infty$ was partially compensated for by using an artificial damping function of the form $\exp[-bs^2]$ (70, 71), where b is a constant whose magnitude depends on s_{max}, and remaining errors were corrected using an integral termination computer calculation.

The radial distribution function, neglecting integral termination corrections, is then given by

$$f(r) = \int_{s=0}^{s\simeq 3} sM_c(s)_{th}\, e^{-bs^2} (\sin sr)ds + \int_{s\simeq 3}^{s_{max}} sM_c(s)_{exp}\, e^{-bs^2} (\sin sr)ds. \qquad (13)$$

Upon the adoption of the internuclear probability function given in reference (72) and the inclusion of a correction for the failure of the Born approximation (73), the $M_c(s)_{th}$ used was calculated by

$$M_c(s)_{th} = \left\{ \sum_i \sum_{j \neq i} Z_i Z_j \exp\left[-(l_\alpha)_{ij}^2 s^2/2\right] (\cos \Delta\rho_{ij}) \right.$$

$$\left. \times (\sin s(r_g(l)_{ij} + \phi(s)_{ij}))/s(r_e)_{ij} \right\} / \sum_k (Z_k^2 + Z_k), \quad (14)$$

where $(l_\alpha)_{ij}$ is the root mean square amplitude of vibration of the ij<u>th</u> atom pair (72), cos $(\Delta\rho_{ij})$ is the correction for the failure of the Born approximation, $r_g(l)_{ij}$ is the center of gravity of the peak in the f(r) curve representing the ij<u>th</u> atom pair, $\phi(s)_{ij}$ is a phase shift caused by the anharmonic vibration of the ij<u>th</u> pair and $(r_e)_{ij}$ is the equilibrium distance of the ij<u>th</u> atom pair. $M(s)_{th}$ was calculated using an identical expression with the exception that μ_{ij} was allowed to vary.

The experimental radial distribution curve is then computed by replacing integrals with summations in Equation 13, giving

$$f(r) = (\pi^2/100) \sum_{q=0}^{q\simeq 10} q_i R M_c(q_i)th \exp(-\pi^2 b q_i^2/100) \sin(\pi q_i r/10)$$

$$+ \sum_{q\simeq 10}^{q_{max}} q_i M_c(q_i)_{exp} \exp(-\pi^2 b q_i^2/100) \sin(\pi q_i r/10) \quad (15)$$

if Δq is taken as unity, where R is a factor, called the index of resolution, which puts $M_c(q)_{th}$ on the same scale as $M_c(q)_{exp}$.

The radial distribution function was then corrected for integral termination errors (74) by addition of

$$T = (R/2) \sum_j [c_j/(r_e)_j] \exp(-H_j s_m^2) (I_- + I_+) \qquad (16)$$

where I_- is $[2H_j s_m \cos(X_j s_m) - X_j \sin(X_j s_m)] / [(2H_j s_m)^2 + X_j^2]$,

I_+ is $[2H_j s_m \cos(p_j s_m) - p_j \sin(p_j s_m)] / [(2H_j s_m)^2 + p_j^2]$,

H_j is $(b + l_j^2/2)$,

s_m is the maximum s value,

X_j is the $|r - (r_e)_j|$,

p_j is $(r + (r_e)_j)$,

and R, b and c are constants.

The anharmonic radial distribution function, f(r), was converted to a nearly harmonic, or Gaussian radial distribution function, $f_c(r)$, by addition of the asymmetry correction (75)

$$A = -k \sum_j c_j a_j l_j / (6(r_e)_j (2b+l_j^2)^{1/2}$$

$$[l_j(r-(r_e)_j)/(2b+l_j^2)]^3 \exp[-(r-(r_e)_j)^2 / (4b+2l_j^2)] \qquad (17)$$

where a_j and c_j are constants for a component peak j, and k is a constant.

The function $f_c(r)$ was then analyzed by minimizing the sum of the squares of $[f(r)_{syn} - f_c(r)]$, where $f(r)_{syn}$ is a synthetic Gaussian function given by

$$f(r)_{syn} = K \sum_j c_j / [r_j(2b+1_j^2)^{1/2}] \exp [-(r-r_j)^2/(4b-21_j^2)] . \quad (18)$$

Parameters resulting from the least squares analysis are the centers of gravity of the harmonic function, $f_c(r)$. Electron diffraction parameters most commonly reported are the center of gravities of the anharmonic radial distribution function and the probability distribution function. Relations between these parameters are (72)

$$r_g(1) \simeq r_c + a1_\alpha^4/(4b + 21_\alpha^2)$$

$$r_g(0) \simeq r_g(1) + 1_\alpha^2/r_e + (3a^2/2r_e - 5a/2r_e^2 + 2/r_e^3)1_\alpha^4$$

where r_c, $r_g(1)$, and $r_g(0)$ are the center of gravities of $f_c(r)$, $f(r)$, and $P(r)$ respectively,

a is the anharmonicity constant,

b is the damping constant and

1_α is the root mean square amplitude of vibration (72).

3. Errors

The experimental uncertainties of the parameters measured by electron diffraction are associated with both systematic and random errors. These uncertainties may be separated into three categories (69). First, there are the systematic errors associated with the determination of the scattering variable, s. The scattering variable, as previously described, is a function of the electron wave length, λ, and the camera length, L; accordingly the error in s is dependent on the error in both L and λ. These errors mainly affect the determination of bond lengths and not so much the vibrational amplitudes.

The second group contains errors associated with the determination of the intensity as a function of the scattering variable. It includes systematic errors, which are due to the uncertainty in the shape of the sector, and random errors, which are due to emulsion irregularities and microphotometer fluctuations. The errors in this group affect the determination of both bond lengths and vibrational amplitudes by approximately the same amount. These errors manifest themselves in the noise level of the radial distribution function and uncertainties in the parameters were assessed according to reference (59) where the standard deviations are given by

$$\sigma(r) = 1.94 \quad \sigma(f) \left[2b + l^2\right]^{1/2}/f_m \qquad (19)$$

and

$$\sigma(l) = 1.33 \quad \sigma(f) \left[2b + l^2\right] / l f_m. \qquad (20)$$

where $\sigma(f)$ is the standard deviation of the least-squares fit of the experimental radial distribution function,

b is the damping constant in $\exp(-bs^2)$,

l is the amplitude of vibration and

f_m is the maximum height of the peak representing the bond r.

A recent study (76) of least-squares techniques used for analyzing electron diffraction data has demonstrated a close agreement between results of the method used for assessing random errors in the present work and the results of more elaborate and rigorous procedures.

The third class of uncertainties consists of systematic errors in the intensity measurements such as improper emulsion calibration and unsuitable correction for extraneous scattering. Errors in this classification mainly affect the degree of damping of the $M(q)_{exp}$ function rather than the nodal positions; therefore they affect the determination of vibrational amplitudes which are related to the envelope of $M(q)_{exp}$ and not the bond lengths. The associated uncertainties in vibrational amplitudes were estimated using the following equation.

$$\sigma_R(1) = .7\ 1\ [\sigma(R)/R] . \qquad (21)$$

where R is the index of resolution, defined as $M(q)_{exp}/M(q)_{th}$ and $\sigma(R)$ is the standard deviation of R.

In the present analysis the uncertainties in the vibrational amplitudes were calculated using Equations 20 and 21. The approximate contributions of the various factors affecting the uncertainties in bond distances are listed in Table 1.

Table 1. Estimated uncertainties in bond lengths for favorable case, parts per thousand (angstrom units)

Source	
Wavelength (λ)	.2
Camera length (L)	.3
Sector shape	.6
Gas spread	.0 - .4
Fit of f(r) curve	.8
Estimated net	1.1

III. STRUCTURAL RESULTS

A. Oxygen

Oxygen was one of several diatomic molecules studied in this laboratory to check the absolute significance of bond lengths determined by electron diffraction (7). Heretofore, the procedure for interpreting electron intensities in terms of rational molecular parameters had never been rigorously tested. The comparison of parameters obtained in this study with accurately known spectroscopic parameters should provide a helpful test of the validity of current electron scattering theory.

A sample of 99.8 per cent pure oxygen was purchased from the Matheson Company. Diffraction data were taken for all three camera distances using sample pressures of approximately 14, 21 and 25 millimeters of mercury and exposure times of approximately 20, 47 and 117 seconds for long, middle and short camera distances respectively. The sample pressures were dictated more by the speed of the vacuum pumps with this noncondensable specimen than by design to avoid multiple scattering.

Four plates for each camera distance were selected for microphotometering and the resulting optical density data were converted to intensities (Figures 2 - 4) as previously outlined. The experimental data used for calculating the radial distribution function (Figure 5) were overlapped at the

Figure 2. A plot of the experimental $I(q)_T$ and I_B functions of the long camera range for oxygen

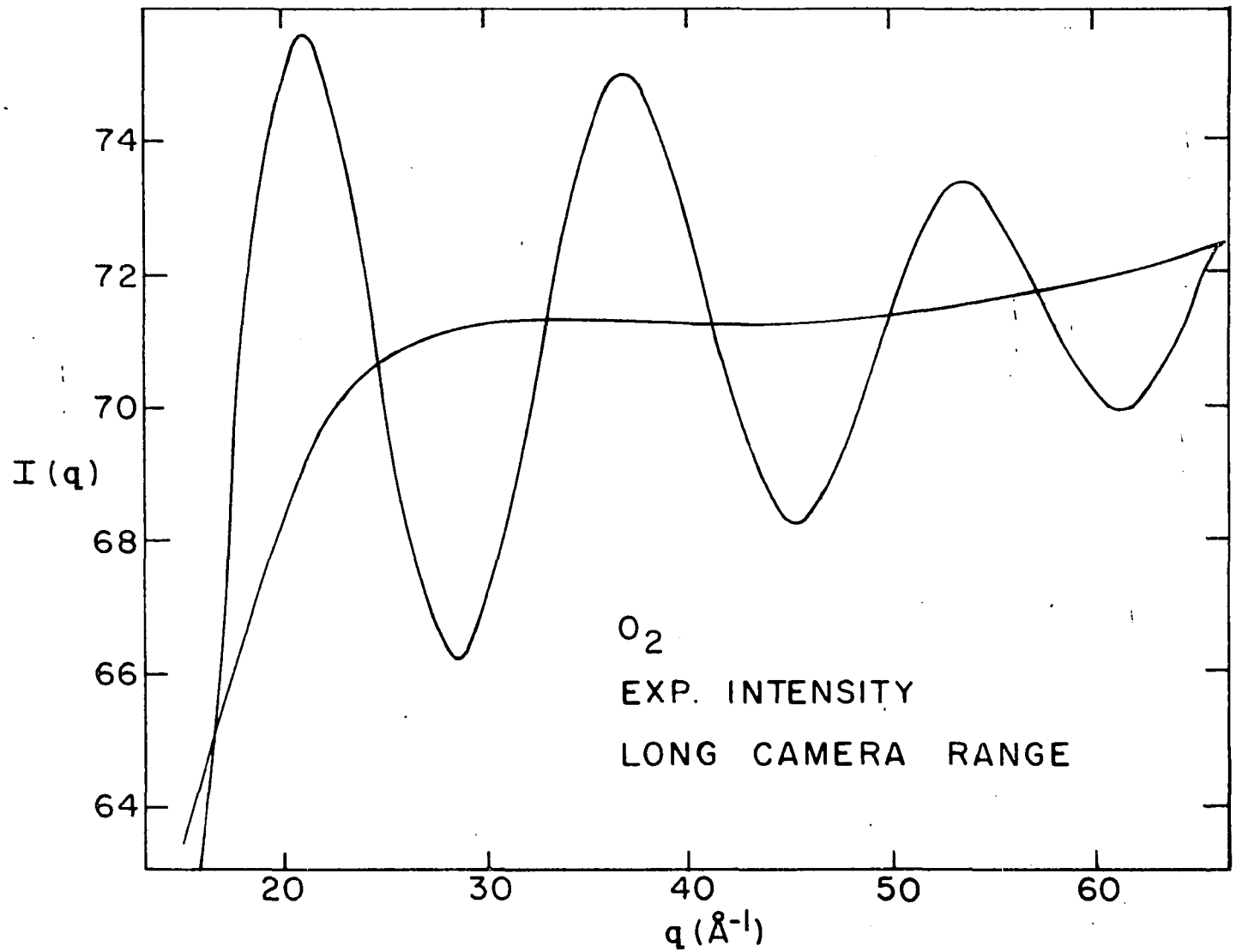
74
72
70
68
66
64
I(q)
20
30
40
50
60
q (Å-1)
O2
EXP. INTENSITY
LONG CAMERA RANGE

Figure 3. A plot of the experimental $I(q)_T$ and I_B functions of the middle camera range for oxygen

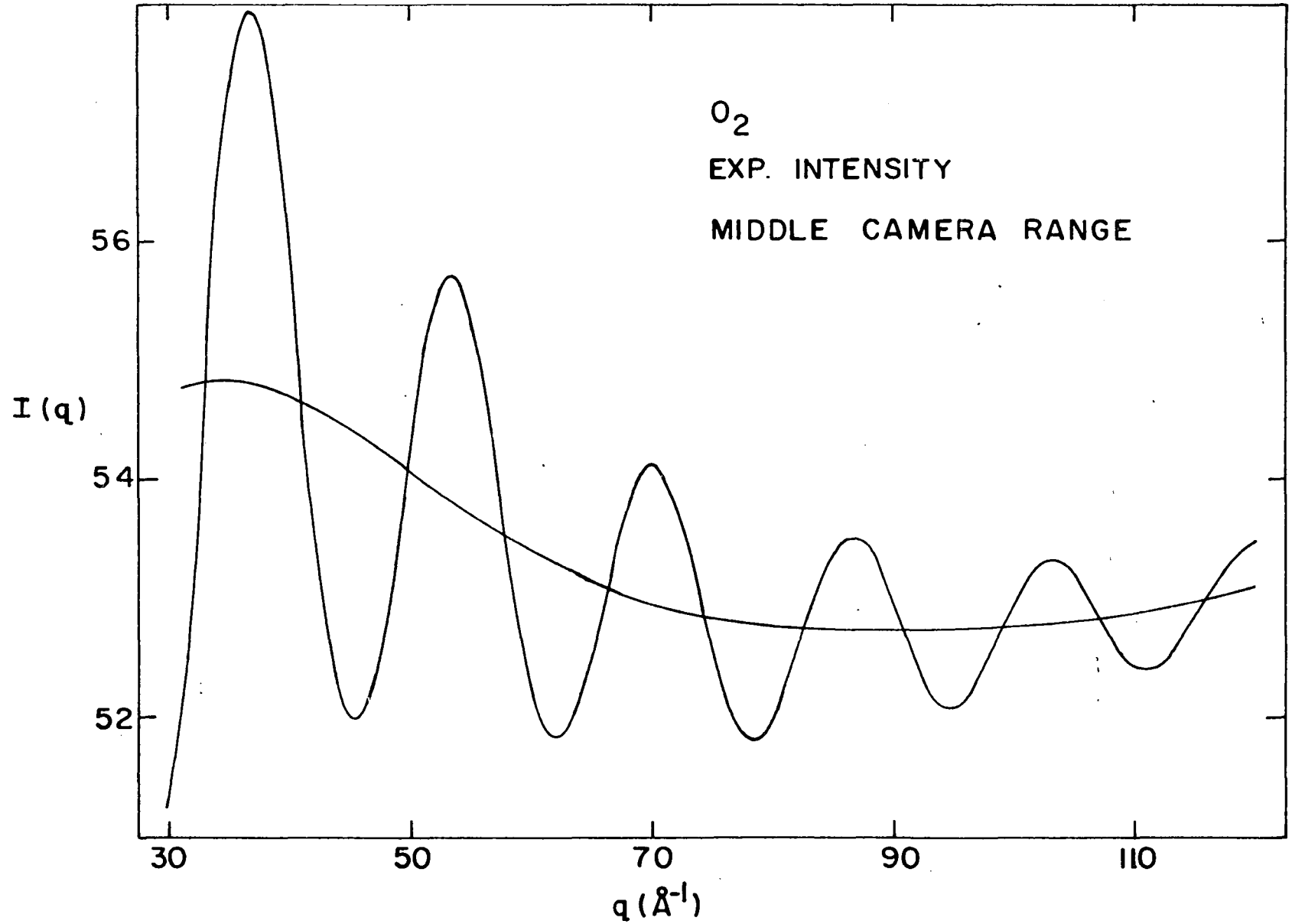
O_2
EXP. INTENSITY
MIDDLE CAMERA RANGE
I(q)
56
54
52
30
50
70
90
110
q (Å^{-1})

Figure 4. A plot of the experimental $I(q)_T$ and I_B functions of the short camera range for oxygen

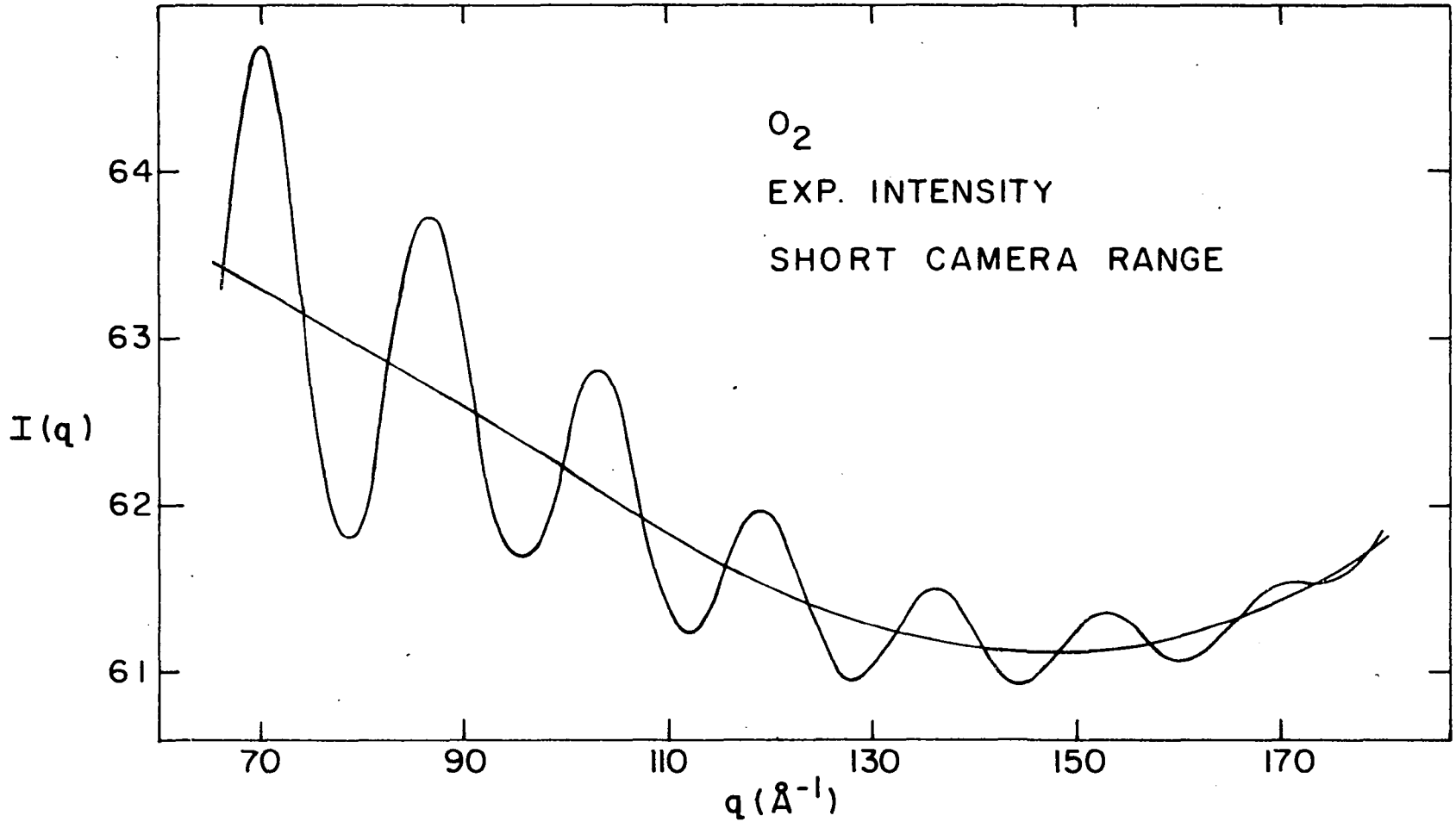
O_2
EXP. INTENSITY
SHORT CAMERA RANGE
I(q)
64
63
62
61
70
90
110
130
150
170
q (Å^{-1})

Figure 5. A plot of the corrected radial distribution function for oxygen. The lower curve is a plot of the difference between experimental and theoretical radial distribution functions

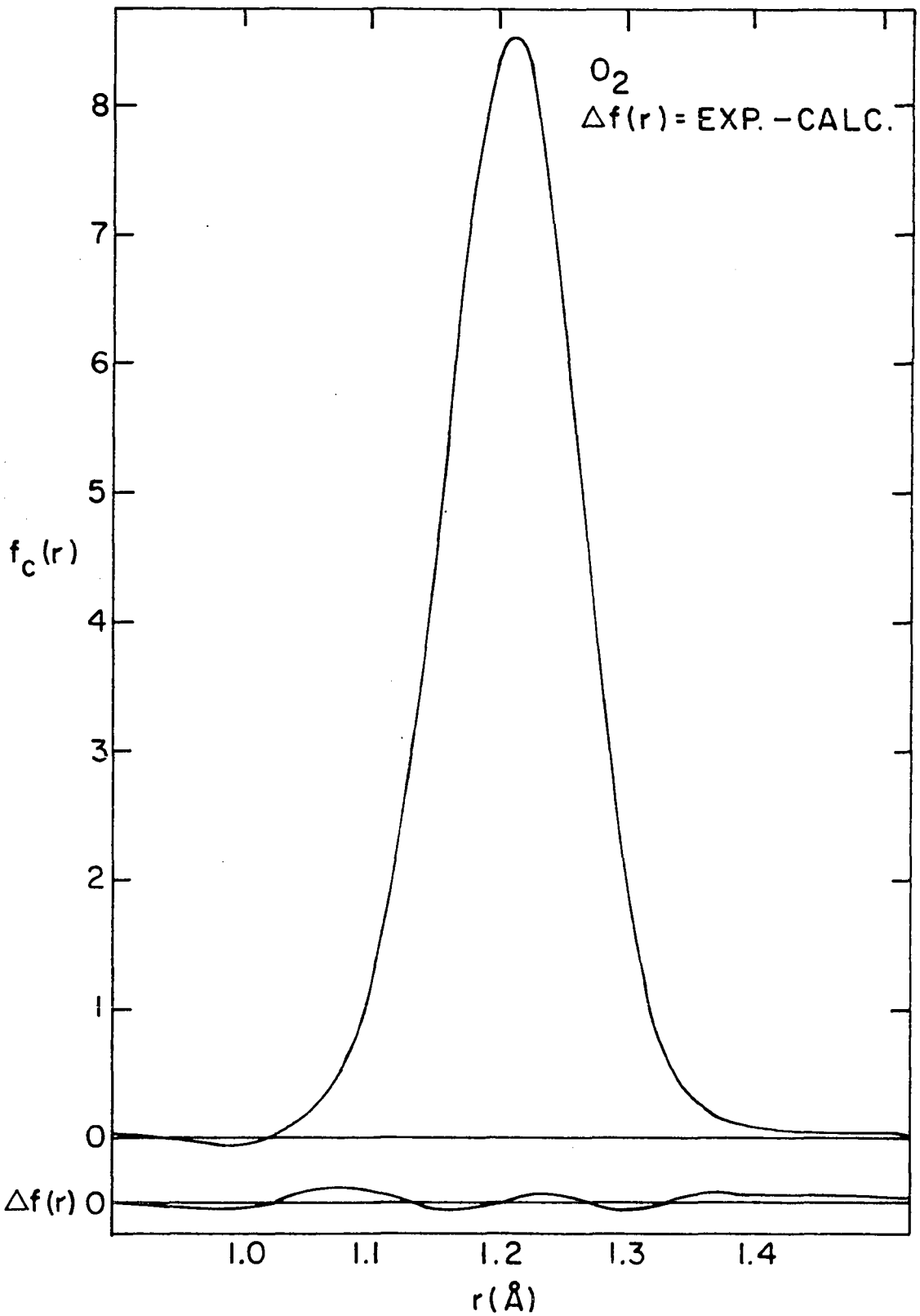
O_2
Δf(r) = EXP. − CALC.
8
7
6
5
4
3
2
1
0
$f_c(r)$
Δf(r) 0
1.0
1.1
1.2
1.3
1.4
r(Å)

points q = 65 and q = 107 and the short data extended to q = 180. Theoretical data was grafted on from q = 0 to q = 16. The analysis of the oxygen data was done using both the IBM 650 and IBM 7074 digital computers.

The center of gravity, $r_g(0)$, and the amplitude of vibration, l_α, resulting from a least-squares fit of the radial distribution function were 1.2129 ± 0.0011 Å and 0.0389 ± 0.0010 Å. If the molecule is assumed to be a Morse oscillator, the distance parameter $r_g(0)$, may be reduced to the equilibrium parameter, r_e, according to reference (72) by the relation

$$r_e = r_g(0) - 3al^2/2 - 13a^3l^4/12 - \delta_{rot}, \qquad (22)$$

where a is the Morse anharmonicity constant and δ_{rot} is a correction for centrifugal stretching (77). The centrifugal correction is given by $2kT/r_eK_e$, where k is the Boltzman constant, T is the absolute temperature, and K_e is the force constant of the bond. When the spectroscopic value of a (78) of 2.4 $Å^{-1}$ was used, the equilibrium internuclear distance calculated was r_e = 1.2074 ± 0.0011 Å. The spectroscopic results for r_e and l_α are 1.2074 Å and 0.037 Å (78). The close agreement between diffraction and spectroscopic results lends support to the present interpretation of absolute significance of the diffraction parameters.

B. Perfluorotetramethylhydrazine

A sample of perfluorotetramethylhydrazine was donated by J. A. Young of the University of Florida. The purity of the sample was approximately 99 per cent as indicated by an accompanying gas phase chromatogram. The liquid appeared cloudy, however, and was distilled to insure purity. The colorless fraction collected at 32 degrees centigrade, the observed boiling point (79), was assumed to be pure perfluorotetramethylhydrazine.

The gas was injected into the diffraction chamber at the vapor pressure of the liquid, 15 millimeters of mercury, at -41 degrees centigrade. The temperature was maintained by using a slush of diethylketone. Long and middle distance photographs were taken and the exposure times used were 2.5 and 7.5 seconds respectively. Four plates for the middle distance and three for the long distance were selected for microphotometering. In the calculation of the radial distribution function theoretical data were used up to $q = 16$ and long distance data were overlapped with middle distance data at $q = 58$, with the data extending to $q = 120$. These intensities are found in Figures 6 and 7. Calculations involved in the analysis of the data were done entirely on the IBM 7074 computer.

Internuclear distances for a given configuration of the molecule were calculated using a computer program supplied

Figure 6. A plot of the experimental $I(q)_T$ and I_B functions of the long camera range for perfluorotetramethylhydrazine

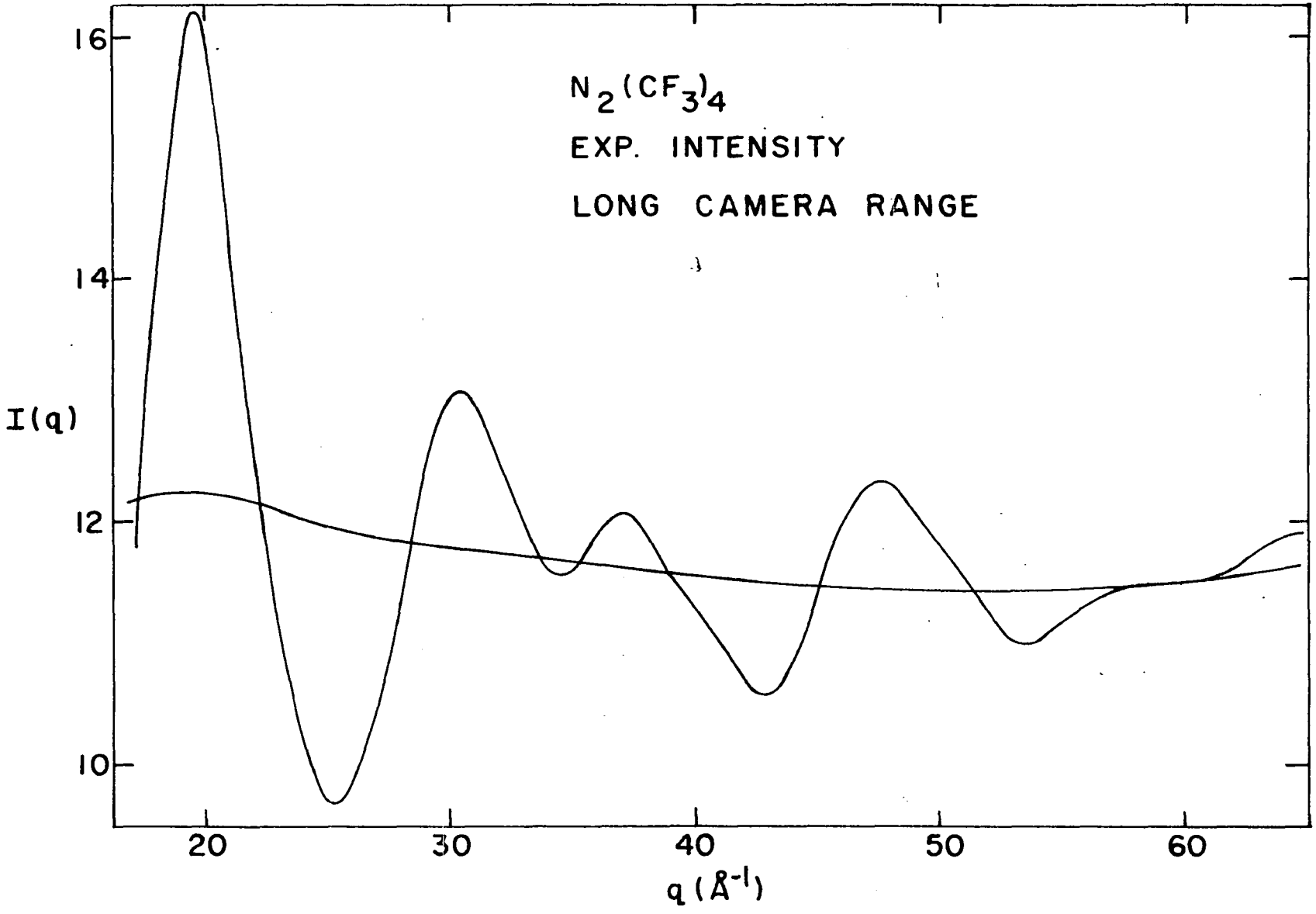
$N_2(CF_3)_4$
EXP. INTENSITY
LONG CAMERA RANGE
I(q)
16
14
12
10
20
30
40
50
60
q (Å^{-1})

Figure 7. A plot of the experimental $I(q)_T$ and I_B functions of the middle camera range for perfluorotetramethylhydrazine

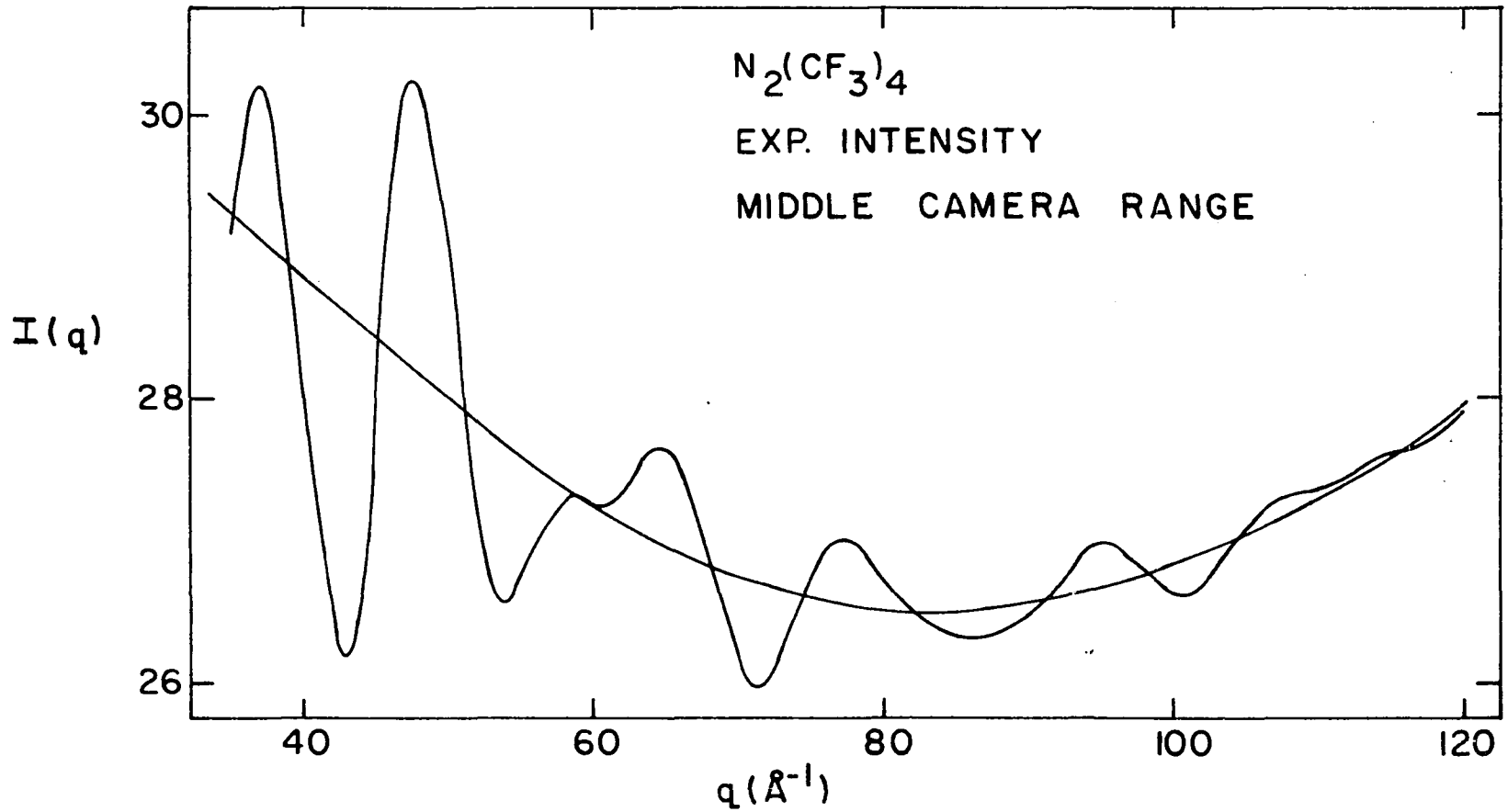
$N_2(CF_3)_4$
EXP. INTENSITY
MIDDLE CAMERA RANGE
I(q)
30
28
26
40
60
80
100
120
q(Å^{-1})

by D. Kohl[1], and theoretical reduced intensity functions were computed with the use of these distances. The features of the preliminary radial distribution functions were quite sensitive to the theoretical model used. This was attributed to the large effect of fluorine-fluorine nonbonded distances upon the $\Delta M_c(q)$ and $M_c(q)_{th}$ functions. To avoid biasing the experimental radial distribution function with the theoretical models assumed in computations of $\Delta M_c(q)$ and $M_c(q)_{th}$, the technique of the Norwegians (80) was applied. A radial distribution function was calculated using data from q_{min} to q_{max} only. The negative region corresponded to the contribution which would have been added to the function had the correct $M_c(q)_{th}$ data been grafted on from $q = 0$ to $q = q_{min}$. The resulting distribution function exhibited a peak around 2.7 Å which was assumed to be the nearest approach of fluorines bonded to different atoms. Because of the complexity of the problem the process used for obtaining an acceptable fit between experimental and theoretical radial distribution functions was one of trial and error. Numerous configurations were tried and eliminated before a reasonably satisfactory theoretical model was found. This model is shown in Figure 8. At this juncture the first peak, which

---

[1]Kohl, D., Chemistry Department, University of Indiana, Generalized computer program for calculation of intramolecular distances. Private communication. 1962.

Figure 8. (a) The carbon nitrogen skeleton of perfluorotetramethylhydrazine as viewed along the N_1 - N_2 axis, (b) A three dimensional drawing of the perfluorotetramethylhydrazine configuration

(a)

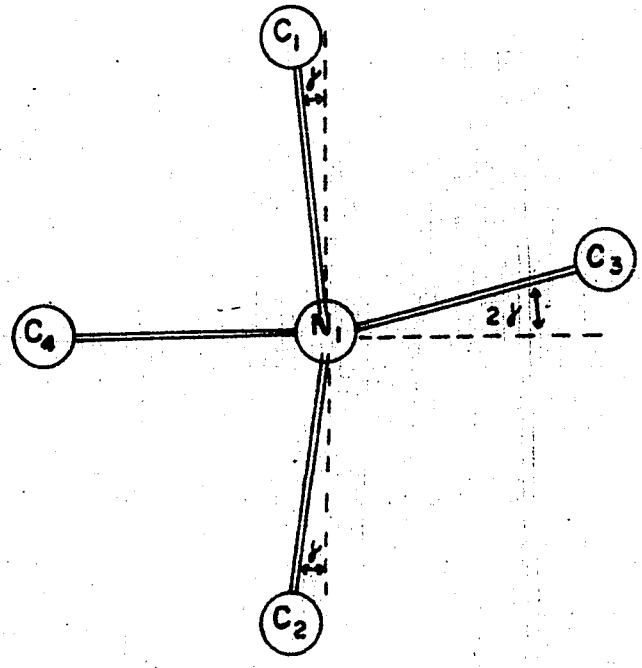
C1
C3
C4
N1
2γ
C2

(b)

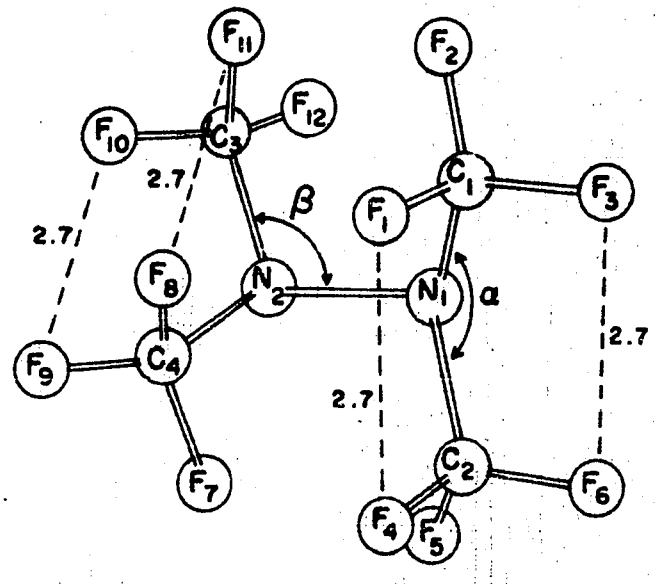
F11
F2
F10
C3
F12
C1
F3
2.7
β
F1
2.7
F8
N2
N1
α
F9
C4
2.7
2.7
F7
C2
F6
F4
F5

Figure 9. A plot of the experimental radial distribution function for perfluorotetramethylhydrazine. Lower curve is the difference between the experimental and theoretical radial distribution functions

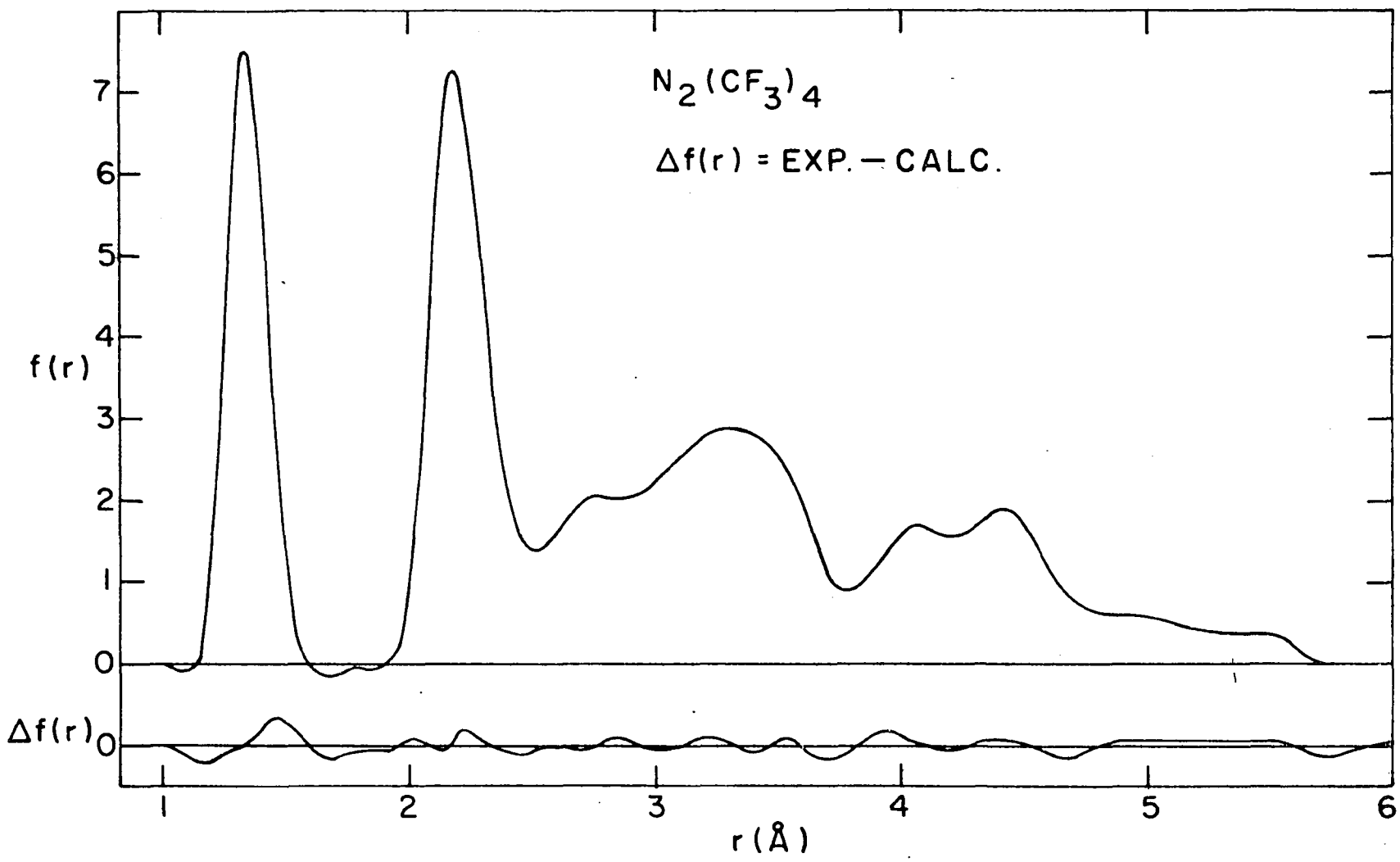
$N_2(CF_3)_4$
Δf(r) = EXP. — CALC.
f(r)
Δf(r)
0
1
2
3
4
5
6
7
r (Å)

contains the bonded distances, and the second peak, which is primarily composed of the shortest F···F and F···N nonbonded distances, were analyzed to obtain mean distances and amplitudes. The angles α, β, γ, of Figure 8 were then found which produced the best fit of experimental and synthetic curves beyond the first two peaks. The relation between these three angles is

$$\gamma = \text{Arc cos } [\sin (\alpha/2)/\sin (180-\beta)] \ . \qquad (23)$$

The procedure used was again one of trial and error. First the angle α which gave the F···F distances of 2.7 Å (see Figure 8) was computed for the case when γ was zero and held constant at this value. Then various β's and their corresponding γ's, as determined by Equation 23, were used to obtain theoretical models. For each of these models the CF_3 groups were rotated about their axis by an appropriate amount in order to maintain the symmetry between the CF_3 groups which are bonded to the same nitrogen atom. This rotation of the methyl groups puts F_2 and F_5 in the plane formed by $C_1N_1C_2$, and F_{12} and F_7 in the plane formed by $C_3N_2C_4$. The parameters which produced the best fit between experimental and synthetic curves are listed in Table 2. The uncertainties reported for the angles α, β and γ represent the changes in the angles which appreciably worsen the fit between the two curves when the previously described symmetry is assumed. The

Table 2. Structural parameters for $N_2(CF_3)_4$

Distance	$r_g(1)$	$\sigma(r)$	l_α	$\sigma(l)$
NN	1.400	0.02 Å	0.050	(assumed)
CN	1.431	0.008 Å	0.041	0.005 Å
CF	1.324	0.003 Å	0.042	0.003 Å

$\angle CNC\ (\alpha) = 121.2^\circ \pm 1.5^\circ$, $\angle FCF = 108.2^\circ \pm 0.5^\circ$,

$\angle NNC\ (\beta) = 119^\circ \pm 1.5^\circ$, $\gamma = 5^\circ \pm 2^\circ$

final radial distribution function is illustrated in Figure 9.

There is no guarantee that the final configuration is unique in fitting the experimental function. However, the large number of configurations tried diminishes the possibility that the structure given in Table 2 is seriously in error.

C. Ethane and Deuterated Ethane

Ethane and deuterated ethane were selected to study the magnitudes of primary and secondary deuterium isotope effects. Using a very crude model of the force field, Bartell (5) had predicted that the secondary isotope effect in ethane might be of the order of 0.003 Å. The accuracy of modern electron diffraction techniques approaches 0.001 Å for simple molecules when systematic and random errors are considered. To enhance the probability of measuring a significant difference the

photographs for the protonated and deuterated species were taken at identical settings of the apparatus. Thus for comparison purposes the systematic errors associated with the apparatus settings would cancel and only random errors would need to be considered.

Samples of ethane and deuterated ethane were purchased from the Phillips Petroleum Company and from Merck, Sharpe and Dohme of Canada Limited, respectively. Both compounds were 99.9 per cent pure and the isotopic purity of the deuterated substance was not less than 98 per cent.

Three independent investigations of both molecules were carried out when it was discovered that random errors other than those previously described were introduced in the first and second determinations. In the first set of data a magnetic disturbance correction associated with the incompletely demagnetized ball bearing race was thought to be constant, but after analyzing the data it was discovered that the sector mounting was slipping inside the race. When the phase of the magnetic disturbance with respect to the sector opening is known, a correction for the effect of the disturbance may be made with accuracy. In the first determination the phase was unknown and an additional random error of approximately 1 part per thousand of the bond distance had to be included. After analyzing the second set of data it was discovered that the sector had been creeping radially along its mounting, thus introducing additional random

error. The maximum error that such a creepage could introduce was calculated and found to be approximately .1 per cent of the bond lengths. A third determination, in which no known large random error occurs, was then done.

The gas was injected into the diffraction chamber at a pressure of 60 millimeters of mercury and the exposure times for the long and middle camera distances were 6 and 20 seconds respectively. Short camera distance data were used in the first study in which the exposure time was 30 seconds. The analyses of ethane and deuterated ethane were carried out using IBM 650 and IBM 7074 digital computers.

In the calculation of the radial distribution function, theoretical intensity data were used up to q = 16 and the long and middle distance data were overlapped at q = 54. The middle data extended to q = 120. When short distance intensity data were used it was overlapped with the middle data at q = 98 and extended to q = 150. Intensity plots for the third analysis are found in Figures 10 - 13. The resulting radial distribution functions are given in Figure 14.

Structural results from each set of ethane data are listed in Table 3 and those for deuterated ethane are listed in Table 4. Weighted mean parameters for each molecule are found in Table 5. These were calculated by

$$\bar{r} = \sum_i w_i r_i / \sum_i w_i$$

where $\bar{r}$ is the weighted mean, r_i is the value obtained from the ith analysis and w_i is a weighting constant for the ith value. The weighting constant used for a particular parameter was assumed to be inversely proportional to the square of the standard deviation of that parameter (81).

Table 3. Molecular parameters for ethane obtained from the radial distribution functions of analysis I, II and III

	Distance	$r_g(1)$	r_e[a]	$\sigma(r)$	l_α	$\sigma(l)$
I.	C-H	1.1039	1.0918	0.0026	0.0789	0.0023
	C-C	1.5323		0.0023	0.0502	0.0020
	C···H	2.1892		0.0050	0.1071	0.0040
II.	C-H	1.1078	1.0911	0.0020	0.0757	0.0016
	C-C	1.5348		0.0020	0.0493	0.0016
	C···H	2.1918		0.0031	0.1060	0.0030
III.	C-H	1.1072	1.0902	0.0017	0.0763	0.0014
	C-C	1.5308		0.0017	0.0484	0.0014
	C···H	2.1866		0.0026	0.1089	0.0022

[a]The r_e values were calculated using Equation 22 but no correction was made for centrifugal stretching.

Figure 10. A plot of the experimental $I(q)_T$ and I_B functions of the long camera range for ethane

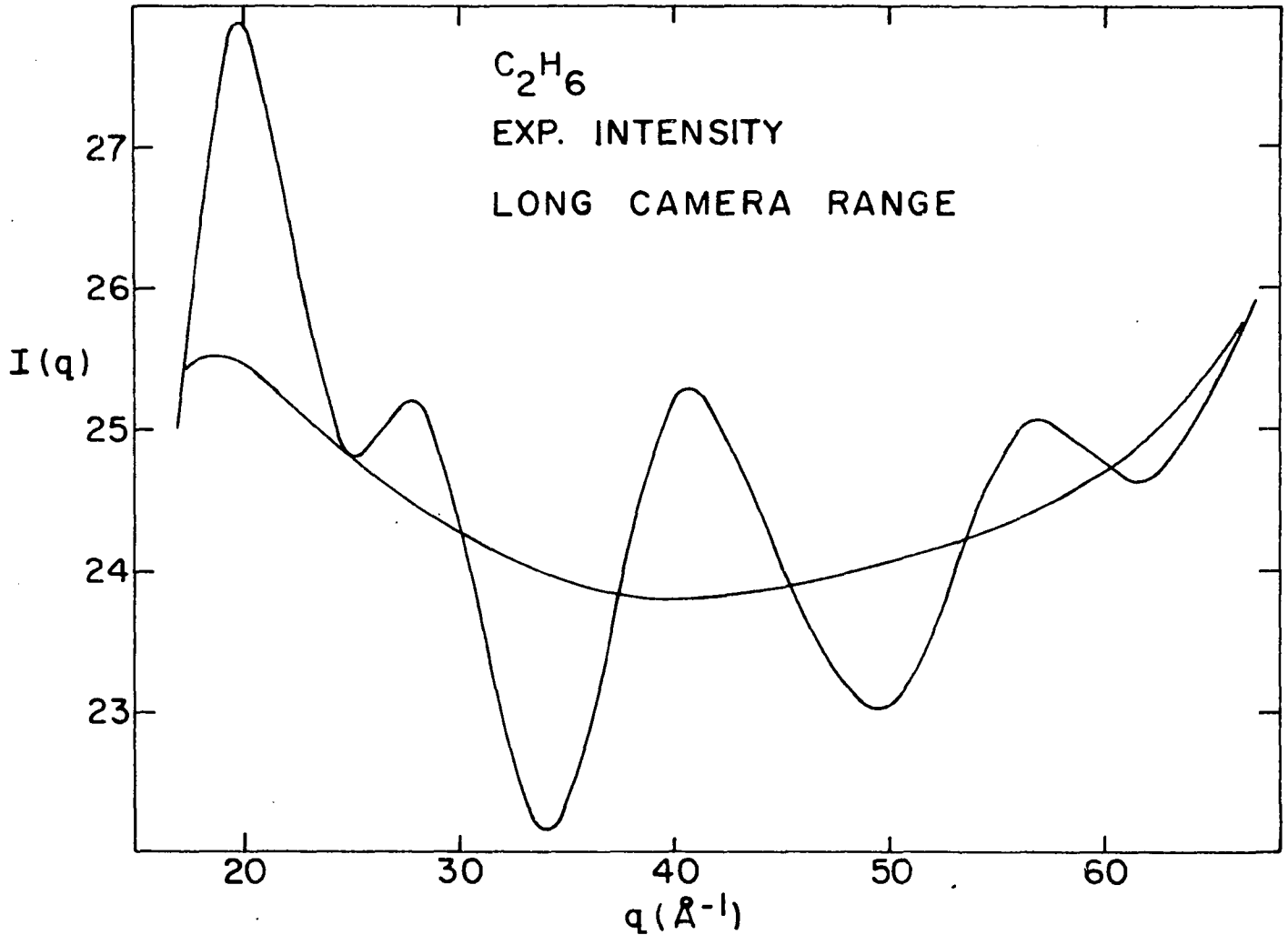
C_2H_6
EXP. INTENSITY
LONG CAMERA RANGE
I(q)
27
26
25
24
23
20
30
40
50
60
q(Å⁻¹)

Figure 11. A plot of the experimental $I(q)_T$ and I_B functions of the middle camera range for ethane

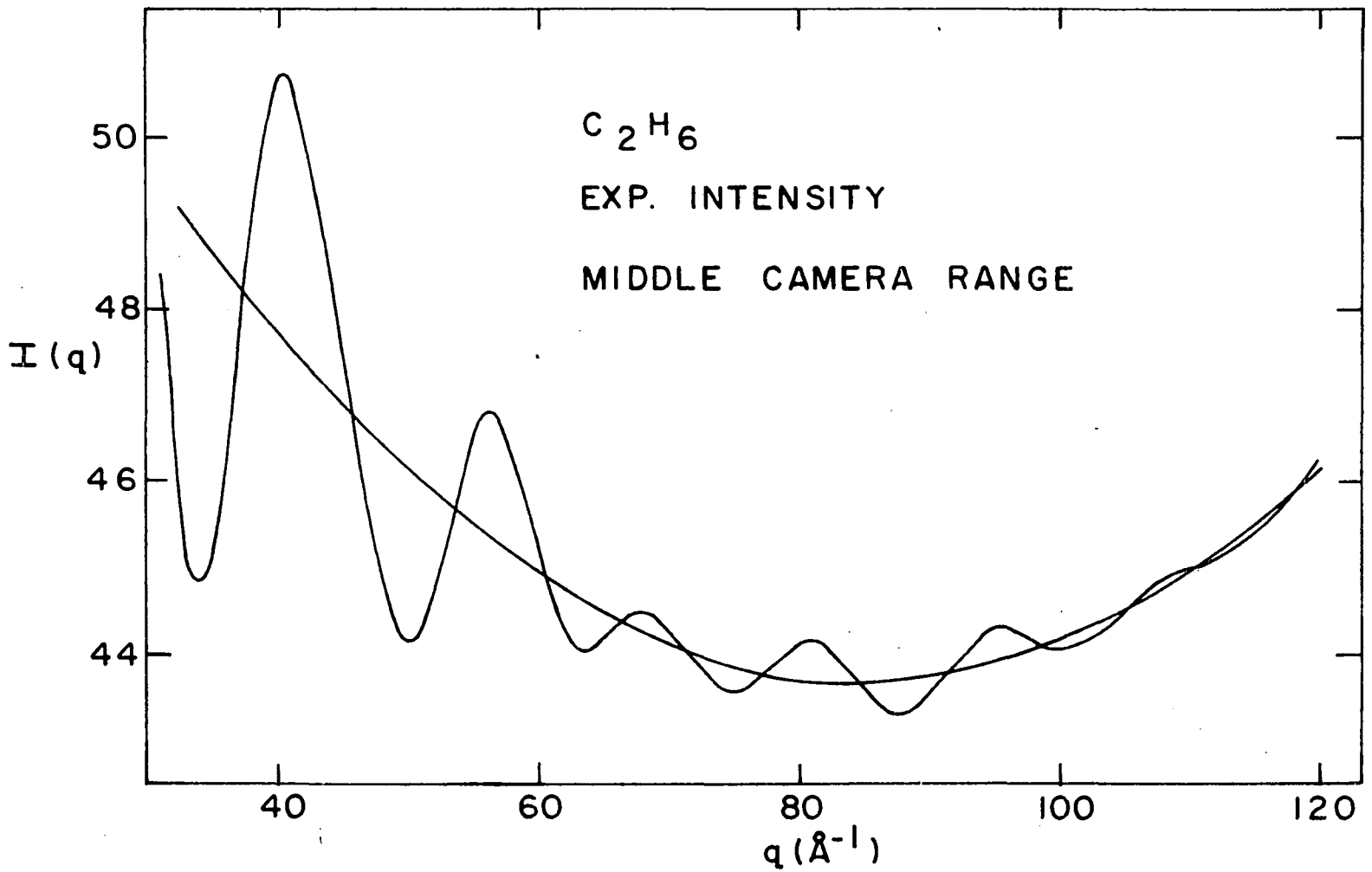
C_2H_6
EXP. INTENSITY
MIDDLE CAMERA RANGE
I(q)
50
48
46
44
40
60
80
100
120
q(Å^{-1})

Figure 12. A plot of the experimental $I(q)_T$ and I_B functions of the long camera range for deuterated ethane

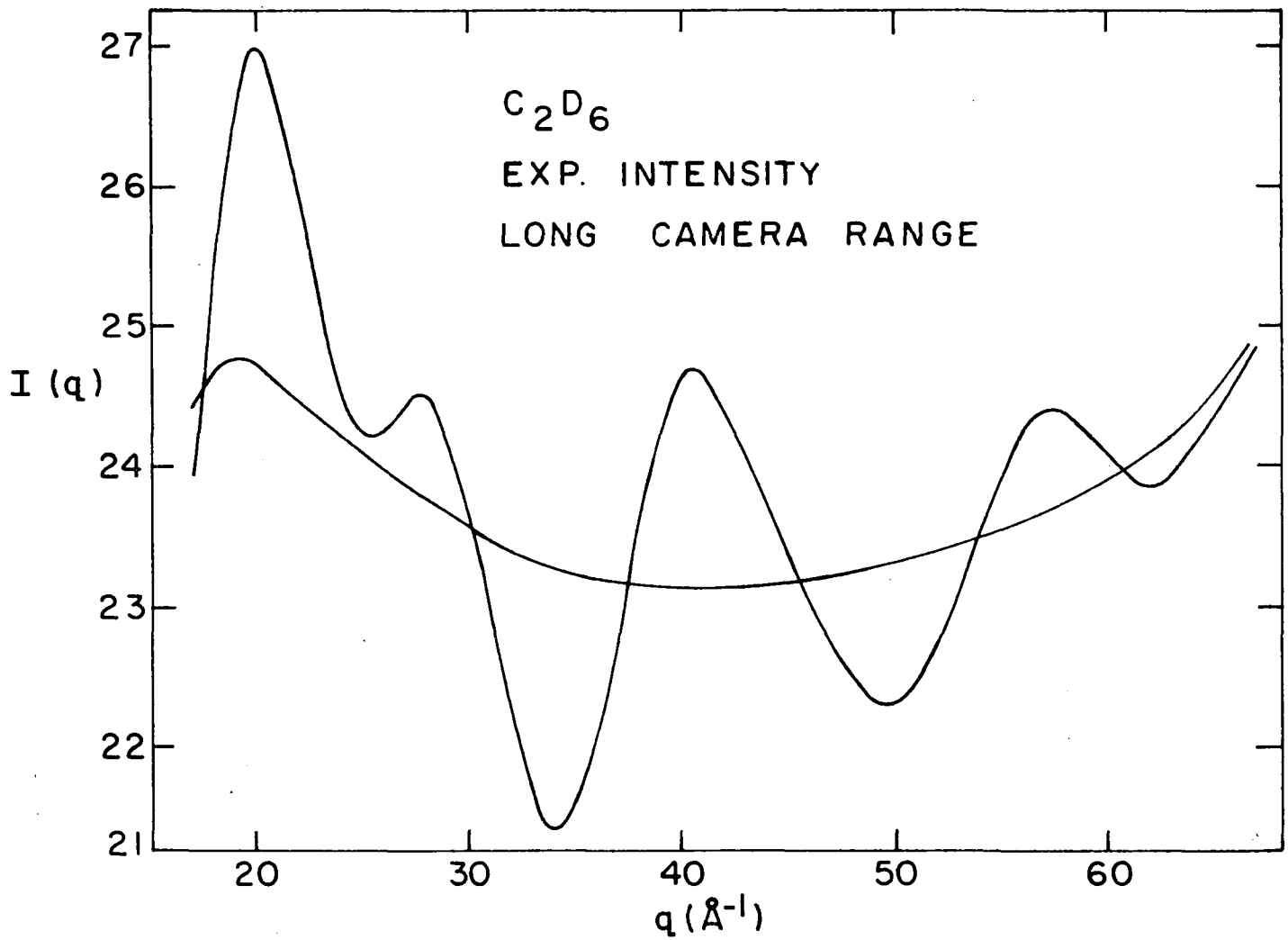
C_2D_6
EXP. INTENSITY
LONG CAMERA RANGE
I (q)
27
26
25
24
23
22
21
20
30
40
50
60
q (Å^{-1})

Figure 13. A plot of the experimental $I(q)_T$ and I_B functions of the middle camera range for deutrated ethane

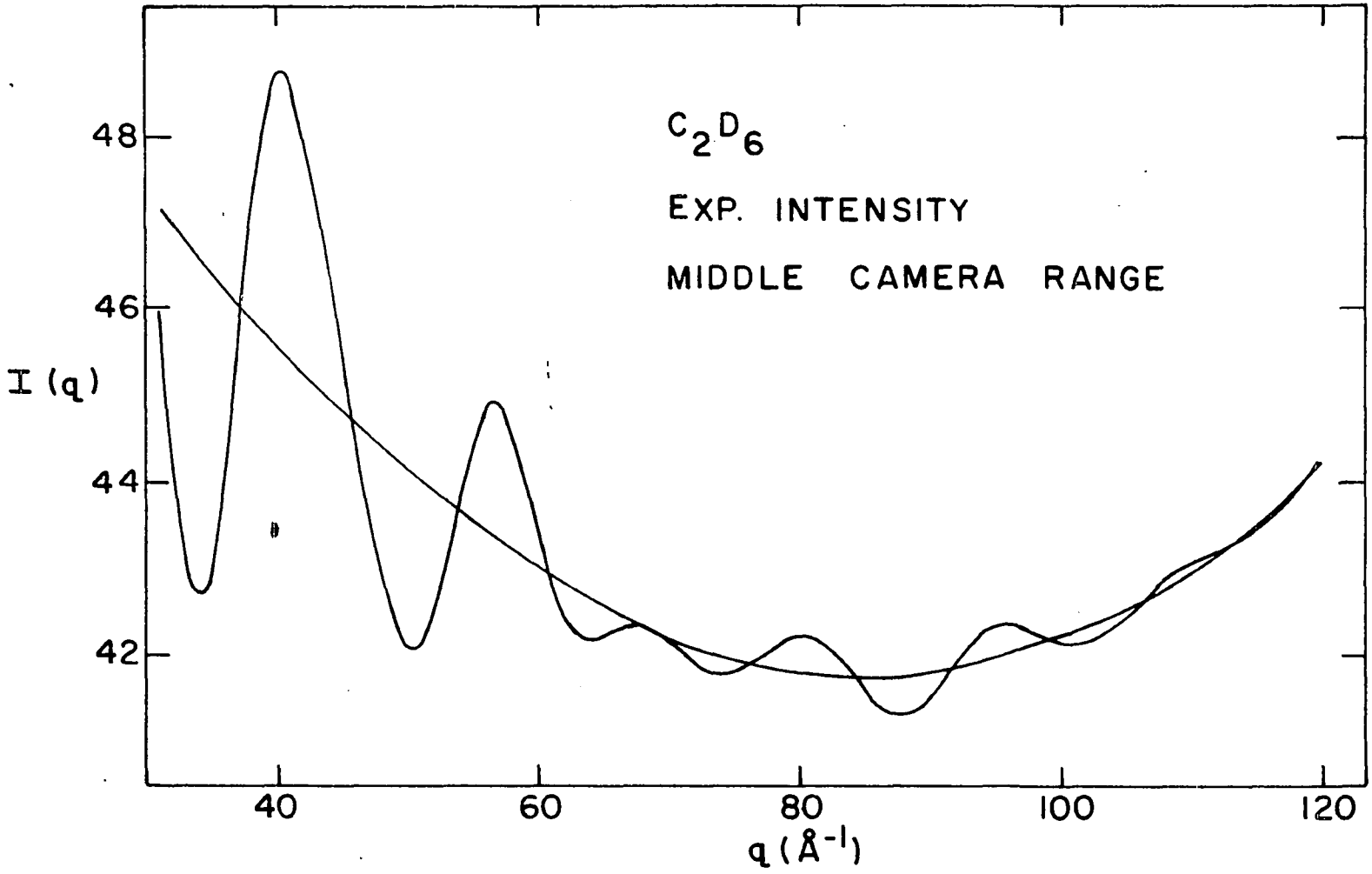
C_2D_6
EXP. INTENSITY
MIDDLE CAMERA RANGE
I (q)
48
46
44
42
40
60
80
100
120
q (Å^{-1})

Figure 14. Corrected radial distribution functions for ethane and deuterated ethane

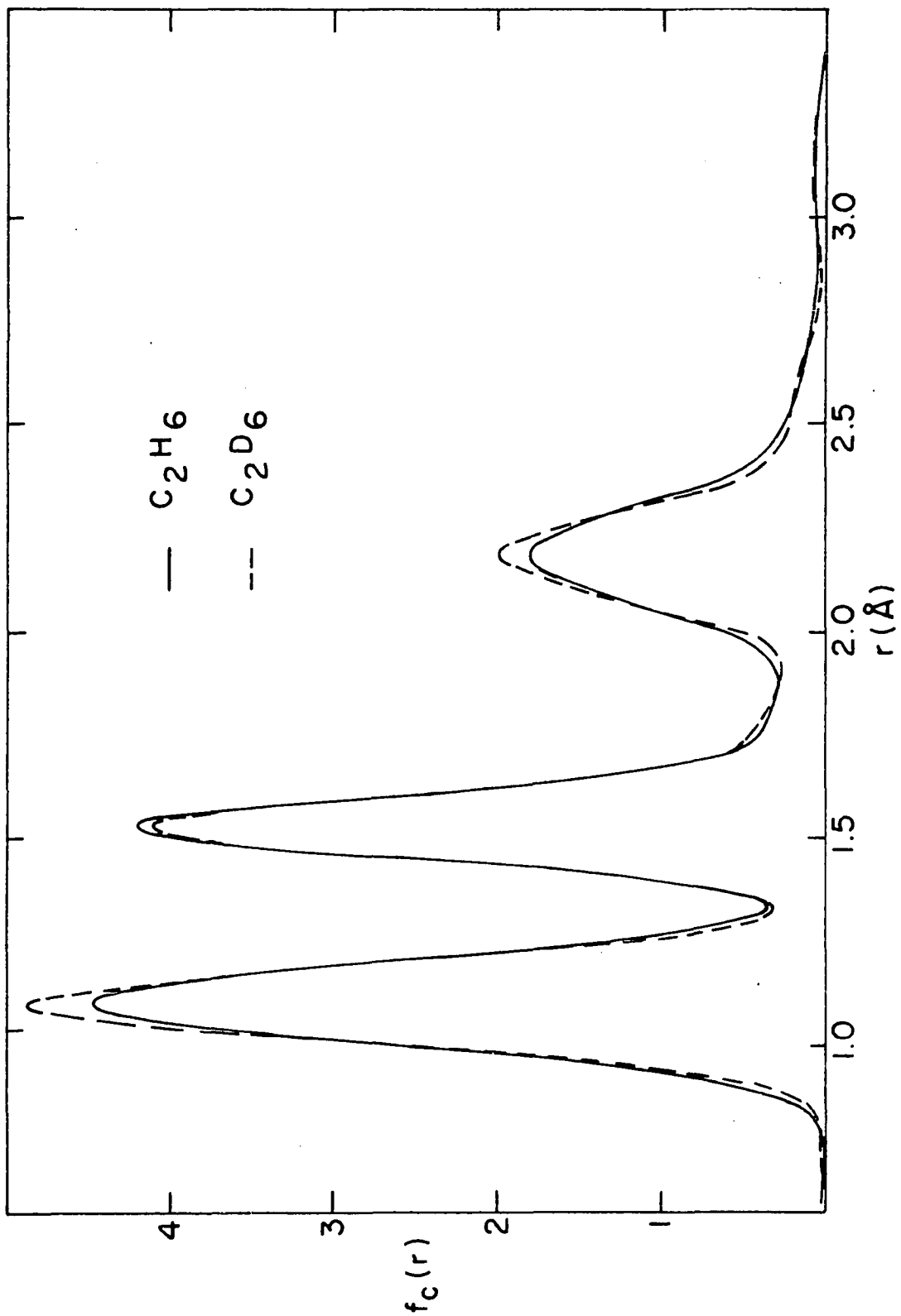
C_2H_6
C_2D_6
$f_c(r)$
r (Å)
1.0
1.5
2.0
2.5
3.0
1
2
3
4

Table 4. Molecular parameters for deuterated ethane obtained from the radial distribution functions of analysis I, II, and III

	Distance	$r_g(1)$	r_e[a]	$\sigma(r)$	l_α	$\sigma(l)$
I.	C-D	1.0990	1.0897	0.0025	0.0694	0.0022
	C-C	1.5288		0.0022	0.0526	0.0020
	C···D	2.1795		0.0033	0.0934	0.0030
II.	C-D	1.1046	1.0914	0.0021	0.0677	0.0018
	C-C	1.5345		0.0022	0.0500	0.0017
	C···D	2.1896		0.0036	0.0949	0.0030
III.	C-D	1.1034	1.0904	0.0017	0.0671	0.0015
	C-C	1.5292		0.0017	0.0512	0.0015
	C···D	2.1836		0.0026	0.0945	0.0024

[a]The r_e values were calculated using Equation 22 but no correction was made for centrifugal stretching.

The radial distribution functions for ethane and deuterated ethane (Figure 14) are clearly different. The greater sharpness of the CD bonded and nonbonded peaks is associated with the smaller amplitudes of vibration of deuterium as compared with hydrogen. This is a consequence of the lower frequency and, hence, the smaller zero point energy of atoms of the heavier isotope. Since the stretching potential energy function is skewed, the smaller amplitudes of vibration of deuterium result in a shorter center of

Table 5. Mean molecular parameters of ethane and deuterated ethane obtained from weighted averages of parameters of analysis I, II, and III

Distance		$r_g(1)$	r_e[a]	$\sigma(r)$	l_α	$\sigma(l)$
C_2H_6	C-H	1.1068	1.0908	0.0012	0.0765	0.0011
	C-C	1.5324		0.0011	0.0491	0.0010
	C···H	2.1888		0.0019	0.1078	0.0016
			$\angle CCH = 111^\circ 2' \pm 11'$			
C_2D_6	C-D	1.1028	1.0905	0.0011	0.0678	0.0010
	C-C	1.5306		0.0011	0.0511	0.0010
	C···H	2.1839		0.0018	0.0736	0.0014
			$\angle CCD = 111^\circ 1' \pm 11'$			

[a]Weighted average of approximate r_e values.

gravity bond distance, $r_g(0)$, for CD than for CH (Table 5). To determine the magnitude of this primary isotope effect a weighted mean of the differences, $(r_g(0)_{CH} - r_g(0)_{CD})$, for each analysis, was obtained. When only random errors were considered this mean value was found to be 0.0050 ± 0.0006 Å and is a significant difference according to Cruickshank's criterion (82).

The secondary isotope effect is less pronounced than the primary effect. A weighted mean of the differences between the C_2H_6 and C_2D_6 CC bond distances was found to be 0.0016 ± 0.0007 Å, which, according to the above criterion,

is of possible significance. It is reasonable to conclude that secondary effects of the order of 10^{-3} Å may very well exist. This is supported by a recent microwave study of deuterated and protonated methyl halides by Schwendeman[1]. The C-X distance, where X is chlorine or bromine, was found to be about 0.001 Å longer in the protonated than in the deuterated species.

D. Methylamine and Deuterated Methylamine

Methylamine and deuterated methylamine samples were purchased from the Matheson Company and from Merck Sharp and Dohme of Canada Limited, respectively. Gas phase chromatograms showed the protonated compound to be 99 per cent pure and the deuterated compound to be 98.5 per cent. The impurity in both cases was found to be the corresponding ammonia. Photographs for both compounds were taken at identical settings of the apparatus so that systematic errors would be the same.

The gas was injected into the diffraction unit at a pressure of 46 millimeters of mercury and at room temperature. The exposure times used were 6 seconds for the long camera distance and approximately 20 seconds for the middle camera distance. The experimental intensity data (Figures 15 - 18)

---

[1]Schwendeman, R. H., Chemistry Department, Michigan State University, Bond distances in methyl halides. Private communication. 1964.

Figure 15. A plot of the experimental $I(q)_T$ and I_B functions of long camera range for methylamine

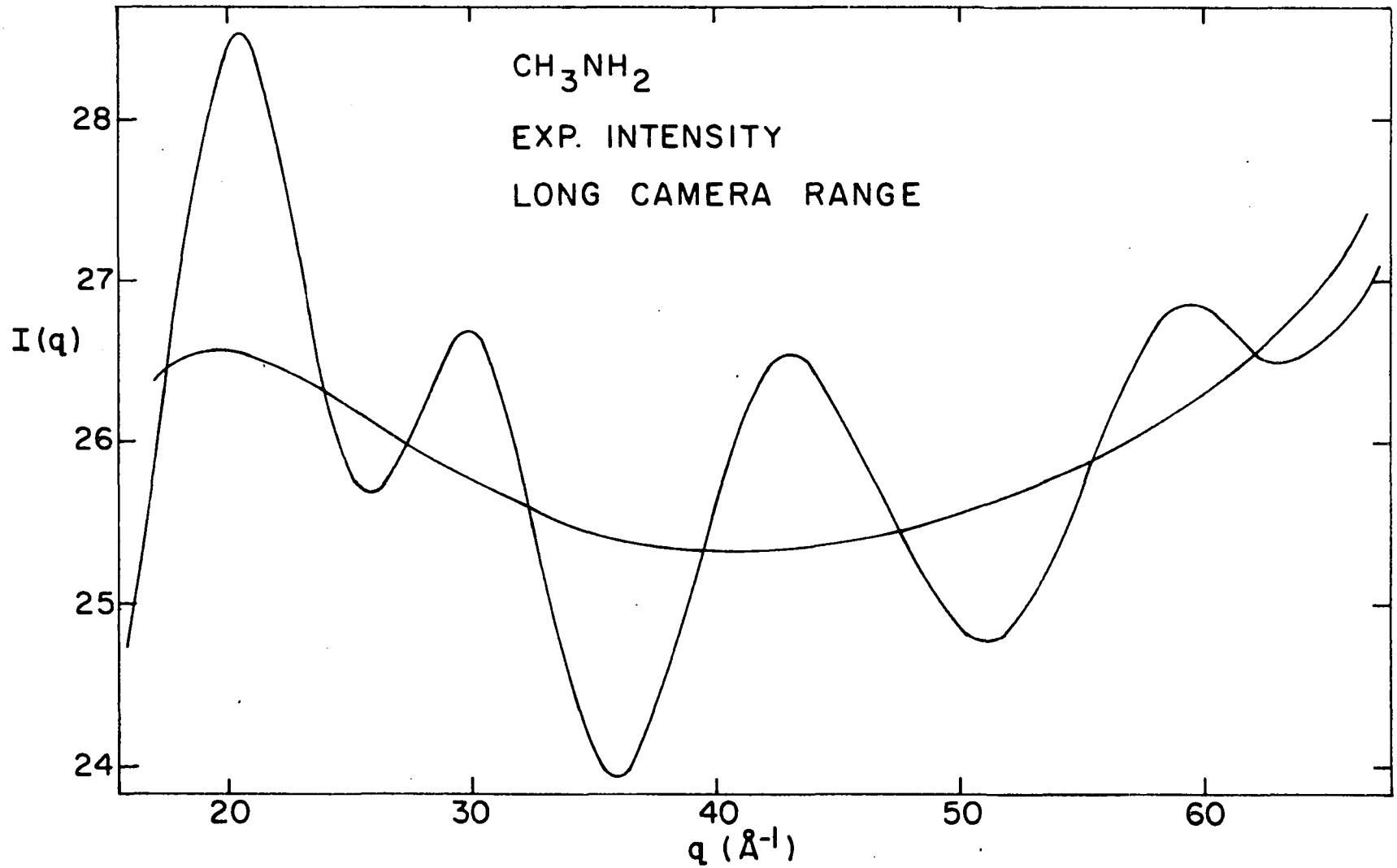
CH_3NH_2
EXP. INTENSITY
LONG CAMERA RANGE
I(q)
28
27
26
25
24
20
30
40
50
60
q (Å^{-1})

Figure 16. A plot of the experimental $I(q)_T$ and I_B functions of the middle camera range for methylamine

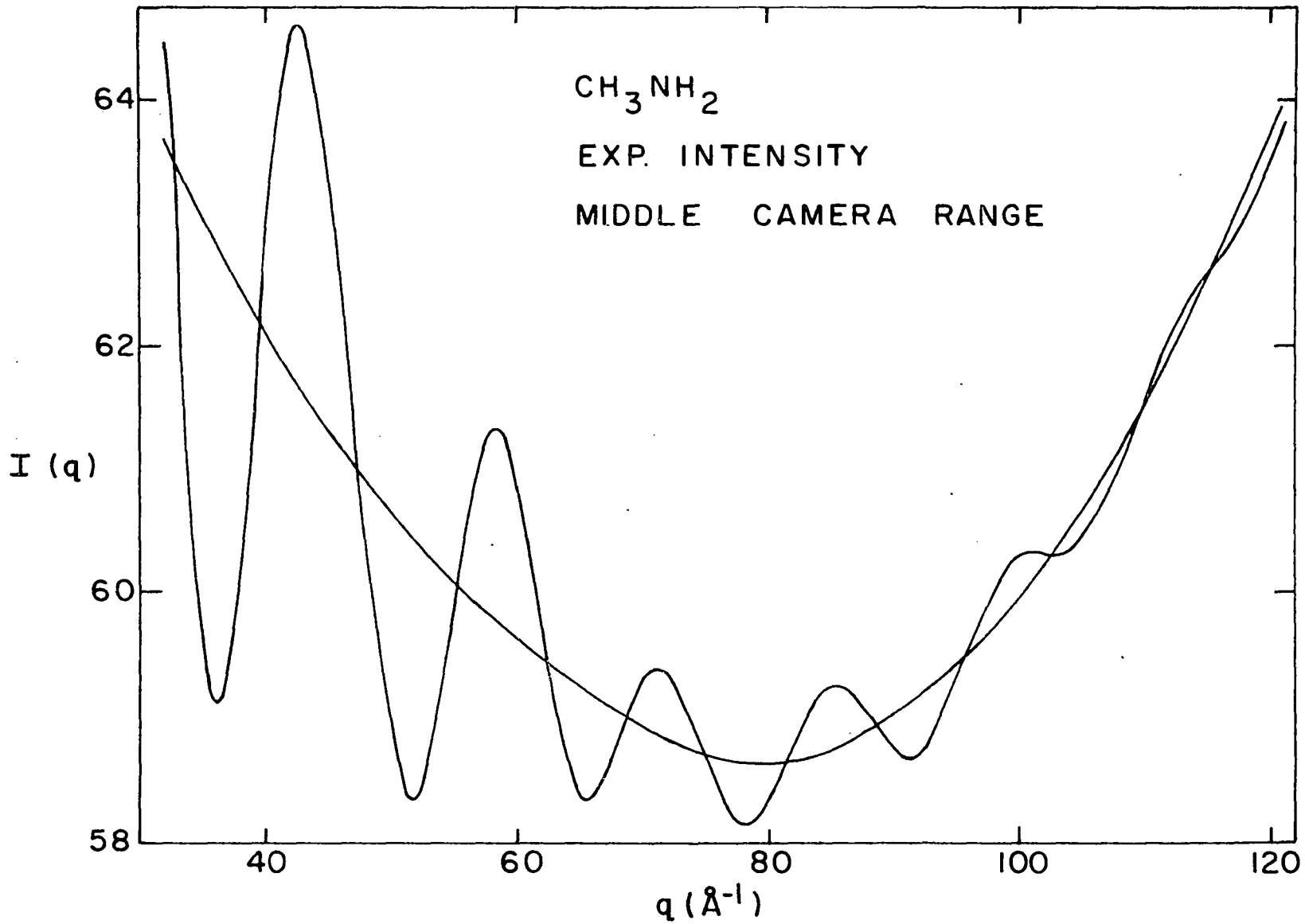
CH_3NH_2
EXP. INTENSITY
MIDDLE CAMERA RANGE
I (q)
64
62
60
58
40
60
80
100
120
q (Å^{-1})

Figure 17. A plot of the experimental $I(q)_T$ and I_B functions of long camera range for deuterated methylamine

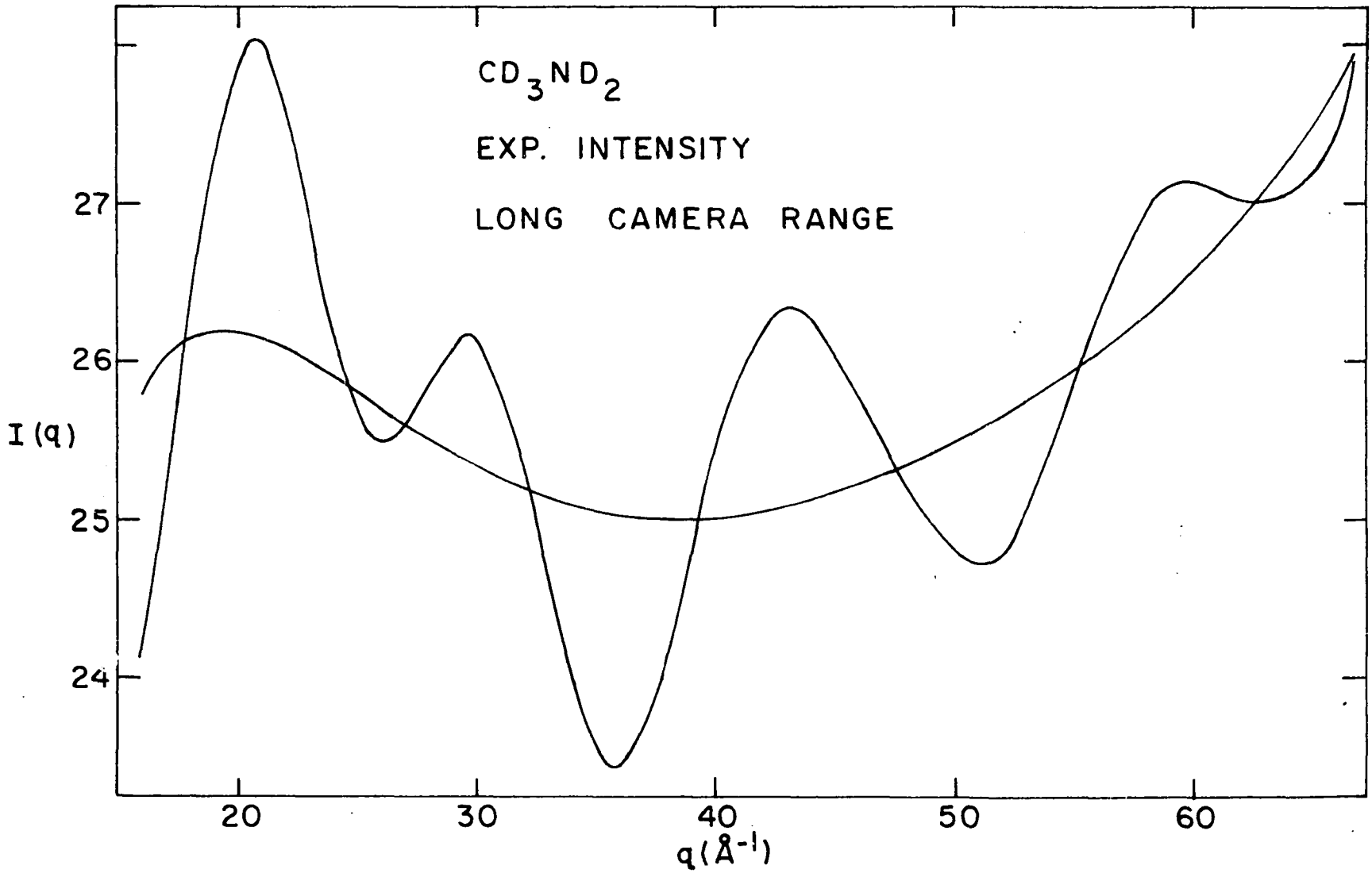
CD_3ND_2
EXP. INTENSITY
LONG CAMERA RANGE
I(q)
27
26
25
24
20
30
40
50
60
q(Å^{-1})

Figure 18. A plot of the experimental $I(q)_T$ and I_B functions of middle camera range for deuterated methylamine

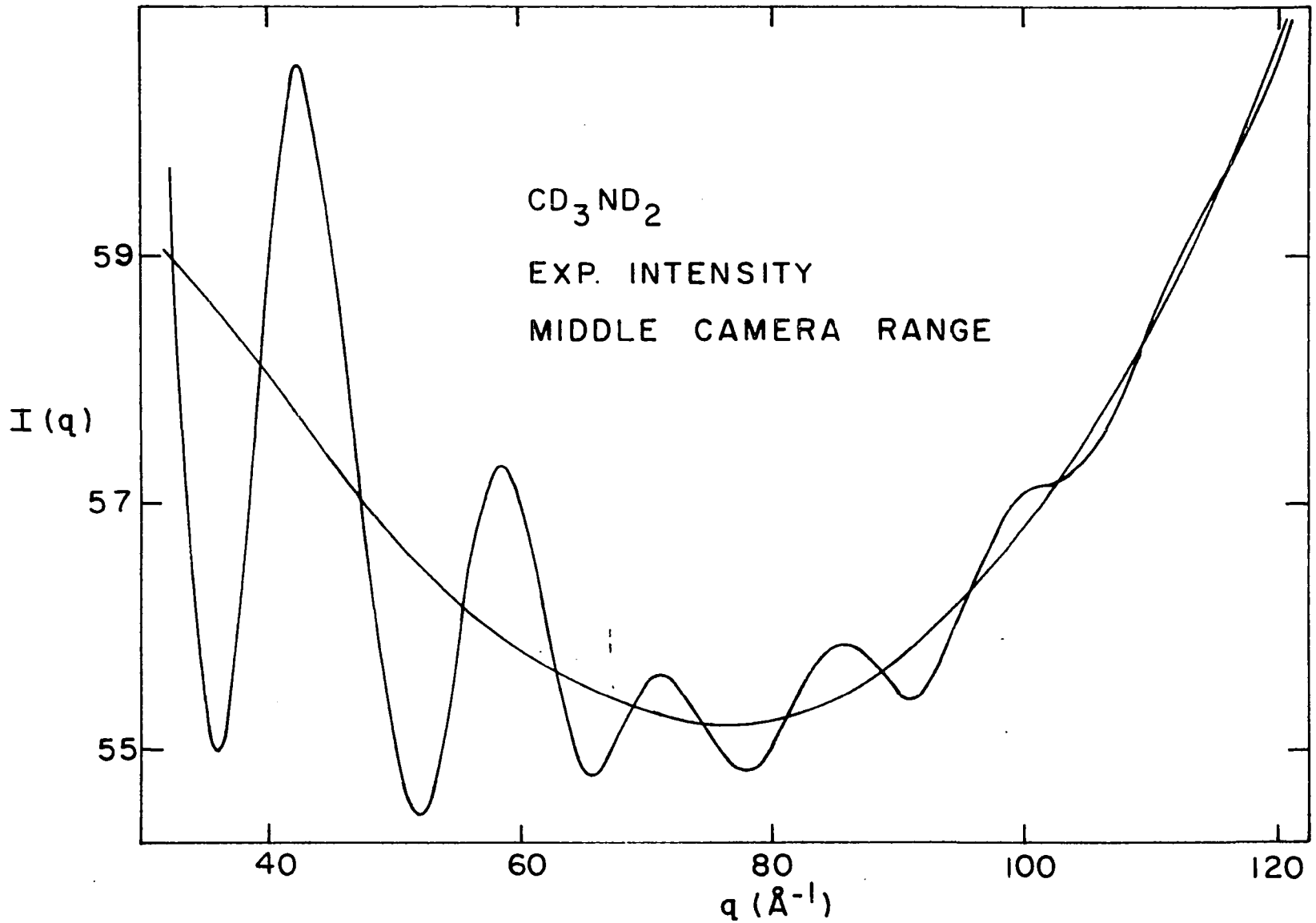
CD_3ND_2
EXP. INTENSITY
MIDDLE CAMERA RANGE
I(q)
59
57
55
40
60
80
100
120
q (Å^{-1})

Figure 19. Corrected radial distribution functions for methylamine and deuterated methylamine

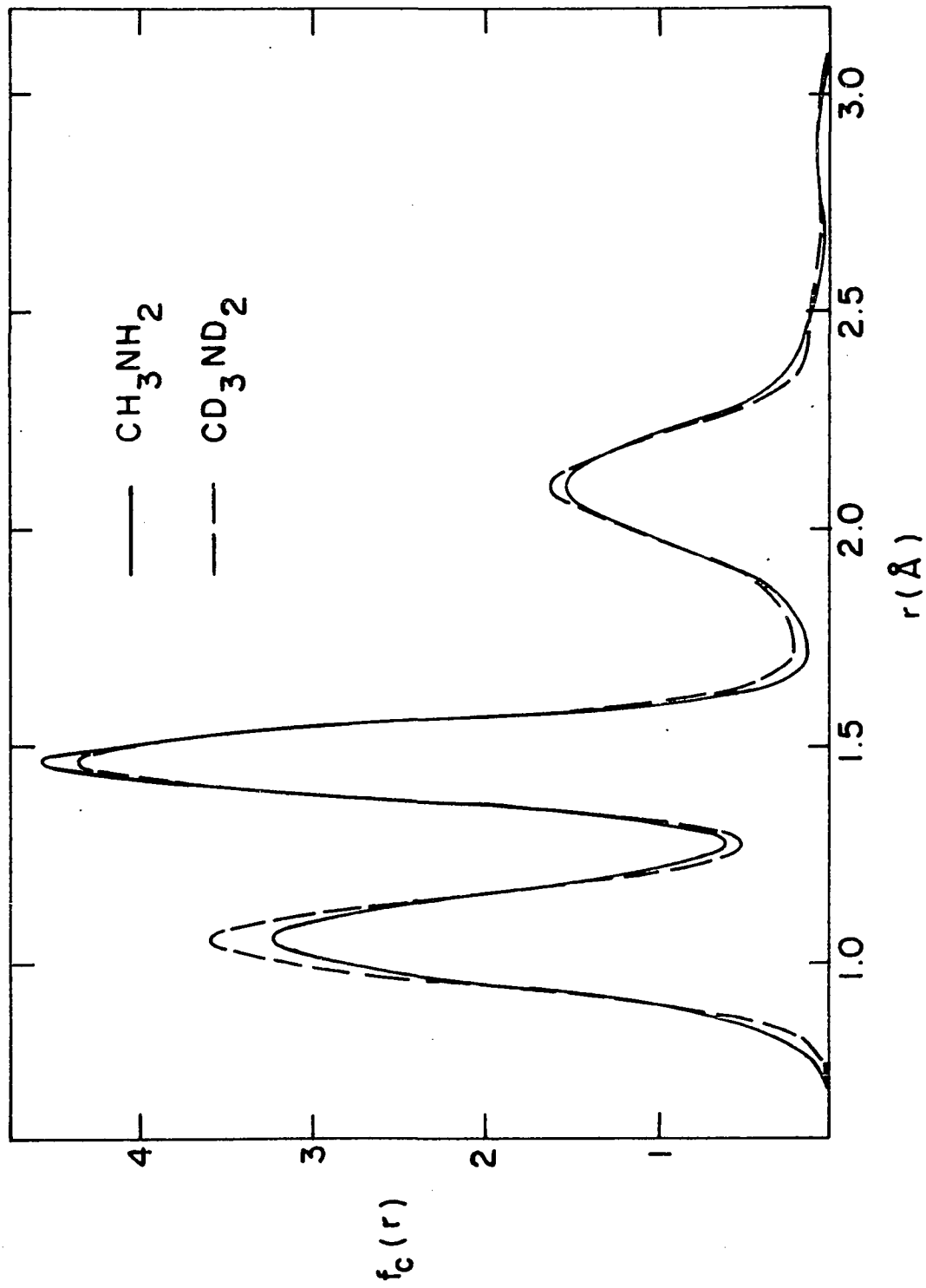
CH_3NH_2
CD_3ND_2
$f_c(r)$
r(Å)
1.0
1.5
2.0
2.5
3.0
1
2
3
4

used for calculation of the radial distribution functions (Figure 19) were overlapped at q = 56 and the middle data extended to q = 120. Theoretical data were grafted on from q = 0 to q = 16. All calculations involved in the analysis of the methylamines were done using the IBM 7074 digital computer.

Three main peaks occur in the radial distribution function of methylamine. The first consists of bonded NH and CH peaks while the third is primarily due to nonbonded NH and CH peaks. In both cases the bond lengths associated with the components are very nearly equal and a least-squares analysis was unable to resolve these small differences accurately. On the other hand, the second peak, which is due to the CN bond distance, was readily characterized by a least-squares analysis. Therefore only the CN parameters were determined uniquely in the present work. For the purposes of the analysis the other parameters were given the values encountered in their ethane and ammonia analogs.

Methylamine and deuterated methylamine photographs were taken during the same period as was the second set of ethane data. The random error introduced by the sector slipping on its mount was therefore included in the standard deviation, $\sigma(r)$. The presence of ammonia impurities in the samples was found to have a negligible effect on the structure analysis.

The parameters determined and those assumed for the methylamine are listed in Table 6. The presence of primary

Table 6. Methylamine and deuterated methylamine structural parameters obtained from the radial distribution function

Molecule	Distance	$r_g(1)$	r_e	$\sigma(r)$	l_α	$\sigma(l)$
CD_3ND_2	CN	1.4661		0.0021	0.0506	0.0016
	CD[a]		1.091		0.066	
	ND[b]		1.012		0.062	
	$\angle CND^b = 112^o3'$			$\angle NDC^c = 109^o28'$		
CH_3NH_2	CN	1.4652		0.0021	0.046	0.0015
	CH[a]		1.091		0.076	
	NH[b]		1.012		0.072	
	$\angle CNH^b = 112^o3'$			$\angle NCH^c = 109^o28'$		

[a]Parameters assumed from ethane and deuterated ethane.

[b]Parameters assumed from NH_3 and ND_3 (83).

[c]Methyl group was assumed to be tetrahedral.

isotope effects are revealed by the relative heights and breadths of the composite CH and NH peaks in the radial distribution curves. A comparison of the CN bond lengths indicates the absence of an appreciable secondary isotope effect, but the uncertainties involved do not eliminate a secondary effect of 0.006 Å or less, according to Cruickshank's criterion (82).

E. Comparison of Structures

The equilibrium bond length of oxygen was found to be 1.2074 ± 0.0011 Å which agrees excellently with the spectroscopic results reported by Tinkham and Strandberg (52) and Babcock and Herzberg (50). These spectroscopic values for r_e are 1.20741 Å and 1.2074 Å. Other values reported for the oxygen bond length are quite similar.

Table 7 contains structural parameters for ethane and methylamine which have been reported by various investigators and Table 8 contains structural parameters for perfluorotetramethylhydrazine and some related compounds. These tables will facilitate comparisons with results of the present study. In most cases unambiguous comparisons are not possible due to the interpretational uncertainties arising because of the different structural methods involved. For example the operational spectroscopic parameter usually reported, r_o, is an average computed from an effective moment of inertia of the ground vibrational state. In general its exact physical interpretation is not known. Electron diffraction workers, on the other hand, often report mean values but some report values corresponding to the peak maximum in the radial distribution curve and some merely report "effective values". In very few instances have the various parameters been reduced to a comparable basis.

Table 7. Comparison of structural results for ethane and methylamine

Molecule	r_{CC}	r_{CH}	∠CCH	r_{CN}	Method	Reference
C_2H_6	1.543[a]	1.102[a]	109.62°[a]		I.R.[b]	(22)
C_2H_6	1.536 ±.016	1.114 ±.027	110.5 ± 3.5°		VED[c]	(20)
C_2H_6	1.5376 ±.003	1.106 ±.006			R[d]	(24)
C_2H_6	1.536 ±.002	1.108[a]	110.1°[a]		I.R.	(25)

[a]Uncertainties not reported.

[b]Infrared method.

[c]Visual electron diffraction method.

[d]Raman method.

Table 7 (Continued).

Molecule	r_{CC}	r_{CH}	∠CCH	r_{CN}	Method	Reference
C_2H_6	1.536[a]	1.107[a]	109.54°[a]		MSED[e]	(23)
C_2H_6	1.5324 ±.0011	1.1068 ±.0012	111°1' ± 11'		MSED	Present study
CH_3NH_2				1.47 (app.)[f]	I.R.	(32)
CH_3NH_2				1.47 ±.01	VED	(45)
CH_3NH_2				1.474 ±.005	M.W.	(43)
CH_3NH_2				1.474[g]	M.W.	(40)
CH_3NH_2				1.465 ±.002	MSED	Present study

[e]Microphotometer-sector electron diffraction method.

[f]Approximate.

[g]Uncertainty less than one per cent.

Table 8. Structural parameters for perfluorotetramethylhydrazine and related compounds

Molecule	r_{NN}	r_{CN}	∠NNC	∠CNC	r_{CF}	∠FCF	Method	Ref.
$N(CH_3)_3$		1.47 ±0.02		108 ± 4°			VED	(85)
$N_2(CH_3)_2H_2$[a]	1.45 ±.03	1.47 ±.03	110 ± 4°	110 ± 4°			VED	(86)
$N(CF_3)_3$		1.43 ±.03		114 ± 3°	1.32 ±.02	108.5 ± 2°	VED	(87)
$N_2(CF_3)_4$	1.40 ±.02	1.431 ±.008	119° ± 1.5	121.2 ± 1.5°	1.324 ±.003	108° 12' ± 31'	MSED	Present study

[a]Parameters reported are for both 1,2-dimethylhydrazine and 1,1-dimethylhydrazine.

For many years 1.5445 Å (84), the CC distance in diamond, has been accepted as the standard CC single bond distance. Bartell (3) has suggested that the diamond value is unrepresentatively long and that the value of 1.533 ± 0.003 Å, which occurs in several normal hydrocarbons, is a preferable standard for most comparison purposes. Stoicheff (24) suggests a value of 1.536 ± 0.003 Å, which is an average value from ethane investigations. The good agreement with the present results corroborates these suggestions. Fairly good agreement is found also between previously reported CH bond lengths and CCH angles and the more precise values obtained in the present study.

The CN bond length of methylamine determined by the present investigation is appreciably smaller than the values reported in the most recent microwave works (43, 40). The difference is approximately 0.01 Å, which is quite large considering that $r_g(1)$ values are often slightly larger than spectroscopic r_o values.

Structural parameters for perfluorotetramethylhydrazine have not been reported prior to this investigation, but some comparisons with related compounds can be made. The bond distances in perfluorotetramethylhydrazine are quite similar to the analogous distances reported for perfluorotrimethylamine, while the distances in these perfluoro derivatives appear to be somewhat shorter than those found in the

corresponding methyl derivatives. These differences are not particularly significant, however, as the uncertainties in the reported bond distances are quite large. There appears to be a trend of increasing CNC angle in the series trimethylamine, 1,1-dimethylamine, perfluorotrimethylamine and perfluorotetramethyl hydrazine. The NNC angle in perfluorotetramethylhydrazine is also larger than that reported for 1,1-dimethylhydrazine. These increases in angles may be due to the increasing size of the groups attached to the nitrogen atoms. The dihedral angle between the planes which bisect each of the CNC angles and pass through the NN bond was found to be $85 \pm 2^{\circ}$ in perfluorotetramethylhydrazine. The analogous angle in ethane is constrained by symmetry to be 60°, but very little is known about this angle in hydrazine and substituted hydrazines.

IV. SUMMARY

The structure of oxygen has been determined to test the absolute significance of modern electron diffraction parameters. The bond length as determined by electron diffraction agreed with spectroscopic results to well within the 1 part per thousand uncertainty of the diffraction parameter. This good agreement indicates that current interpretational schemes are quite valid for diatomics, and it is reasonable to conclude that mean distances for polyatomic molecules can be obtained with comparable accuracy when the f(r) peaks are widely separated.

Perfluorotetramethylhydrazine has been studied to determine its configuration. The bond distances in perfluorotetramethylhydrazine were found to be in general agreement with those for related compounds. Considerable bond angle distortion was observed as the molecule deformed to minimize its energy. The CNC and the NNC angles in perfluorotetramethylhydrazine were found to be $121.2 \pm 1.5^{\circ}$ and $119 \pm 1.5^{\circ}$, while the analogous angles reported for 1,1-dimethylhydrazine were both $110 \pm 4^{\circ}$. The dihedral angle of the carbon nitrogen skeleton was found to be 85°. The nearest approach of fluorines bonded to different atoms was found to be 2.7 Å, a value which appears to be encountered quite generally in fluorine compounds.

Ethane, methylamine and their deuterated analogs have been investigated to determine the magnitudes of primary and

secondary isotope effects on bond lengths. Three individual studies of the ethanes have been carried out and found to be in agreement to within estimated uncertainties. The analysis gave a primary deuterium effect of 0.0050 ± 0.0006 Å and suggested the presence of a weaker secondary effect of 0.0016 ± 0.0007 Å. Unambiguously defined electron diffraction structural parameters for ethane, with uncertainties of ± 0.0011 Å, have been reported for the first time. The parameters obtained were in reasonably good agreement with previously reported but less precise results. Primary isotope effects in the methylamines were evident in the radial distribution functions, but the magnitude was not determined individually for NH and CH bonds because the bond lengths were too close to be resolved. No secondary isotope effect in the methylamines was observed but the larger uncertainty in the determination did not eliminate an effect of 0.006 Å or less. The CN bond length determined was appreciably smaller than those reported for recent microwave investigations.

V. LITERATURE CITED

1. Dewar, M. J. S., Tetrahedron 17, 123 (1962).
2. Bartell, L. S., J. Chem. Phys. 32, 827 (1960).
3. Bartell, L. S., J. Am. Chem. Soc. 81, 3497 (1959).
4. Bartell, L. S., Tetrahedron 17, 177 (1962).
5. Bartell, L. S., Iowa State J. of Sci. 36, 137 (1961).
6. Bartell, L. S., J. Am. Chem. Soc. 83, 3567 (1961).
7. Bartell, L. S. and Kuchitsu, K., J. Phys. Soc. Japan 17 B-11, 20 (1962).
8. Pauling, L., Nature of the chemical bond, 3rd ed., Ithaca, New York, Cornell University Press, 1960.
9. Buck, F. A. M. and Livingston, R. L., J. Chem. Phys. 18, 570 (1950).
10. Bunn, C. W., Trans. Farad. Soc. 35, 482 (1939).
11. Bunn, C. W. and Howells, E. R., Nature 174, 549 (1954).
12. Moreno, Y., Iijima, T. and Murata, Y., Bull. Chem. Soc. Japan 33, 46 (1949).
13. Coblentz, W. W. Investigations of infra-red spectra. Washington, D. C., Carnegie Institution of Washington. 1905-1908.
14. Levin, A. and Meyer, C. F., J. Opt. Soc. Am. 16, 137 (1928).
15. Crawford, B. L., Avery, W. H. and Linnett, J. W., J. Chem. Phys. 6, 682 (1938).
16. Stitt, F., J. Chem. Phys. 7, 297 (1939).
17. Wierl, R., Ann. Physik 13, 453 (1932).
18. Bauer, S. H., J. Chem. Phys. 4, 407 (1936).
19. Pauling, L. and Brockway, L. O., J. Am. Chem. Soc. 59, 1223 (1937).

20. Hedberg, K. and Shomaker, V., J. Am. Chem. Soc. 73, 1482 (1951).

21. Smith, L. G., J. Chem. Phys. 17, 139 (1949).

22. Hansen, G. E. and Dennison, D. M., J. Chem. Phys. 20, 313 (1952).

23. Almenningen, A. and Bastiansen, O., Acta Chem. Scand. 9, 815 (1955).

24. Stoicheff, B. P., Can. J. Phys. 40, 358 (1962).

25. Lafferty, W. J. and Plyler, E. K., J. Chem. Phys. 37, 2688 (1962).

26. Lafferty, W. J. and Plyler, E. K., J. Research Natl. Bur. Standards A67, 225 (1963).

27. Thompson, H. W. and Skinner, H. A., J. Chem. Phys. 6, 775 (1938).

28. Cleaves, A. P. and Plyler, E. K., J. Chem. Phys. 7, 563 (1939).

29. Kirby-Smith, J. S. and Bonner, L. G., J. Chem. Phys. 7, 880 (1939).

30. Kirby-Smith, J. S. and Bonner, L. G., Phys. Rev. 55, 1113A (1939).

31. Bailey, C. R., Carson, S. C. and Daly, E. F., Proc. Roy. Soc. London 173, 339 (1939).

32. Thompson, H. W., J. Chem. Phys. 7, 448 (1939).

33. Owens, R. G. and Barker, E. F., J. Chem. Phys. 8, 229 (1940).

34. Hershberger, W. D. and Turkevich, J., Phys. Rev. 71, 554 (1947).

35. Gordy, W., Revs. Modern Phys. 20, 668 (1948).

36. Edwards, H. D., Gillian, O. R. and Gordy, W., Phys. Rev. 76, 196 (1949).

37. Lide, D. R., Jr., J. Chem. Phys. 20, 1812 (1952).

38. Lide, D. R., Jr., J. Chem. Phys. 21, 571 (1953).

39. Lide, D. R., Jr., J. Chem. Phys. 22, 1613 (1954).

40. Lide, D. R., Jr., J. Chem. Phys. 27, 343 (1957).

41. Shimoda, K., Nishikawa, T. and Itoh, T., J. Phys. Soc. Japan 9, 974 (1954).

42. Shimoda, K., Nishikawa, T. and Itoh, T., J. Chem. Phys. 22, 1456 (1954).

43. Shimoda, K., Nishikawa, T. and Itoh, T., J. Chem. Phys. 23, 1735 (1955).

44. Itoh, T., J. Phys. Soc. Japan 11, 264 (1956).

45. Allen, P. W. and Sutton, L. E., Acta Cryst. 3, 46 (1950).

46. Ossenbrüggen, W., Z. Physik 49, 167 (1928).

47. Rasetti, F., Phys. Rev. 34, 367 (1929).

48. Curry, J. and Herzberg, G., Ann. Physik 19, 800 (1934).

49. Gajewski, H., Physik. Z. 33, 122 (1932).

50. Babcock, H. O. and Herzberg, L., Astrophys. J. 108, 167 (1948).

51. Townes, S. L. and Miller, C. H., Phys. Rev. 90, 537 (1953).

52. Tinkham, M., Strandberg, M. W. P., Phys. Rev. 97, 951 (1955).

53. Karle, I. L., J. Chem. Phys. 23, 1739 (1955).

54. Hazeldine, R. N., J. Chem. Soc., 102 (1951).

55. Young, J. A., Willian, S. D. and Dresdner, R. O., J. Am. Chem. Soc. 81, 1587 (1959).

56. Brockway, L. O. and Bartell, L. S., Rev. Sci. Instr. 25, 569 (1954).

57. Degard, D., Pierard, J. and Van der Grinten, W., Nature 136, 142 (1935).

58. Debye, P. J. W., Math. and Phys. 4, 133 (1925).

59. Bonham, R. A. and Bartell, L. S., J. Chem. Phys. 31, 702 (1959).

60. Karle, J. and Karle, I. L., J. Chem. Phys. 18, 957 (1950).

61. Bartell, L. S., Brockway, L. O., J. Appl. Phys. 24, 656 (1953).

62. Hauptman, H. and Karle, J., Phys. Rev. 77, 491 (1950).

63. Bewilogua, L., Physik. Z. 32, 740 (1931).

64. Pauling, L. and Brockway, L. D., J. Chem. Phys. 2, 867 (1934).

65. Pauling, L. and Brockway, L. O., J. Am. Chem. Soc. 57, 2684 (1935).

66. Zernike, F. and Prins, J. A., Z. Physik 41, 184 (1927).

67. Viervoll, H., Acta Chem. Scand. 1, 120 (1947).

68. Karle, I. L. and Karle, J., J. Chem. Phys. 17, 1052 (1949).

69. Bartell, L. S., Brockway, L. O. and Schwendeman, R. H., J. Chem. Phys. 23, 1854 (1955).

70. Degard, C., Bull. Soc. Roy. Sci. Liége 6, 383 (1937).

71. Waser, J. and Schomaker, V., Rev. Modern Phys. 25, 671 (1953).

72. Kuchitsu, K. and Bartell, L. S., J. Chem. Phys. 35, 1945 (1961).

73. Bonham, R. A. and Ukaji, T., J. Chem. Phys. 36, 72 (1962).

74. Bartell, L. S. and Brockway, L. O., J. Chem. Phys. 32, 512 (1960).

75. Bonham, R. A., An electron diffraction investigation of free hydrocarbon molecules, unpublished Ph.D. thesis, Ames, Iowa, Library, Iowa State University of Science and Technology, 1958.

76. Morino, Y., Kuchitsu, K. and Murata, Y., (Abstract), Acta Cryst. 16, A129 (1963).

77. Bartell, L. S., J. Chem. Phys. 23, 1219 (1955).

78. Herzberg, G., Spectra of diatomic molecules, 2nd ed., New York, N. Y., D. Van Nostrand Company, Inc., 1950.

79. Dacy, J. R. and Young, D. M., J. Chem. Phys. 23, 13002 (1955).

80. Viervoll, H., Acta Chem. Scand. 1, 120 (1947).

81. Scarborough, J. B. Numerical mathematical analysis. 2nd ed. Baltimore, Maryland, The Johns Hopkins Press. 1950.

82. Cruickshank, D. W., J. Acta Cryst. 2, 65 (1949).

83. Benedict, W. S. and Plyler, E. K., Can. J. Phys. 35, 1235 (1957).

84. Lonsdale, K., Phil. Trans. Roy. Soc. London A240, 219 (1947).

85. Brockway, L. O. and Jenkins, H. O., J. Am. Chem. Soc. 58, 2036 (1936).

86. Beamer, W. H., J. Am. Chem. Soc. 70, 2979 (1948).

87. Livingston, R. L. and Vaughan, G., J. Am. Chem. Soc. 78, 4866 (1956).

VI. ACKNOWLEDGMENTS

I wish to thank Professor L. S. Bartell for the continued guidance and assistance he has given during the course of this research.

I am indebted to Nick Magnani, Ben Carroll and Jack Guillory for their generous help and many suggestions.

For his many helpful discussions, I wish to thank Dr. H. B. Thompson.

Finally, thanks to my wife, to whom I dedicate this work, for typing the rough draft of the thesis and for her moral support throughout this study.